Master's thesis

NTNU
Norwegian University of Science and Technology
Faculty of Engineering
Department of Civil and Environmental Engineering

Arne Bryne Norbotn

Mapping of hazardous areas with geophysical data and geotechnical investigations

Master's thesis in Civil and Environmental Engineering
Supervisor: Rao Martand Singh
June 2023

NTNU
Norwegian University of
Science and Technology

Arne Bryne Norbotn

Mapping of hazardous areas with geophysical data and geotechnical investigations

Master's thesis in Civil and Environmental Engineering
Supervisor: Rao Martand Singh
June 2023

Norwegian University of Science and Technology
Faculty of Engineering
Department of Civil and Environmental Engineering

NTNU
Norwegian University of Science and Technology

Preface

This paper is a master's thesis in geotechnical engineering at the Norwegian University of Science and Technology (NTNU) and the final part of the MSc program in Civil and Environmental Engineering. The work was carried out during the spring semester of 2023. The main supervisor of the thesis has been Rao Martand Sing.

Trondheim, June 2023

Acknowledgement

I would like to thank the following people and institution for their help in my master's thesis:

Professor Rao Martand Singh - For being my supervisor during the project and providing assistance throughout the semester.

Norway's national geological survey (NGU) - For making this project possible and available as a thesis.

Sofie Gradmann (NGU) and Inger-Lise Solberg (NGU) - For providing data as well as continued support and guidance throgout the whole project period.

Espen Andersen Torsæter (NTNU) - For allowing me to participate in fieldwork as well as providing help regarding both field and lab work.

Abstract

Mapping hazardous areas that contain sensitive and potentially unstable soil is a crucial endeavor aimed at reducing the risk of landslides. The fatal consequences of a quick clay landslide was seen clearly in Gjerdrum in 2020. This shows how important it is to try to contain and control areas with unstable soil. In order to achieve this it is important to work on new methods as well as further develop the existing methods to explore and interpret ground conditions. By doing this the risk of material and human loss is can be reduced or ideally avoided.

This project located in Orkdal (south-west of Trondheim) focuses on investigating the effectiveness of a geophysical method called Electrical Resistivity Tomography (ERT) for mapping such areas. It is a project between Norway's national geological survey (NGU), The Norwegian Water Resources and Energy Directorate (NVE) and Norwegian University of Science and Technology (NTNU).

ERT involves injecting current into the ground through electrodes placed in the soil. These electrodes capture the resulting resistivity measurements from the ground, which are then used to generate a 2D map of the subsurface based on the resistivity values. It's important to note that this mapping technique solely relies on resistivity measurements and does not consider other factors related to soil layering.

By combining these geophysical measurements with various geotechnical investigations, it was possible to compare the level of detail provided by the geophysical results. The geophysical mapping, based solely on resistivity values, successfully identified the locations of sensitive areas.

While it was observed that not all areas flagged as potentially sensitive by the geophysical results turned out to be so, it was consistent that all actual sensitive areas were correctly identified by the geophysical method. This suggests that geophysical mapping, such as ERT, has the potential to effectively narrow down possible hazardous areas.

The findings of this project provide supporting evidence for the feasibility of utilizing geophysical mapping techniques to identify and delineate hazardous areas, thereby contributing to improved risk assessment and mitigation strategies for landslides.

Sammendrag

Kartlegging av farlige områder som inneholder sensitiv og potensielt ustabil jord er en avgjørende innsats for å redusere risikoen for skred. De fatale konsekvensene av kvikkleireskred ble tydelig sett i Gjerdrum i 2020. Dette viser bare hvor viktig det er å prøve å begrense og kontrollere områder med ustabil jord. For å oppnå dette er det viktig å jobbe med nye metoder samt videreutvikle eksisterende metoder. Ved å gjøre dette kan risikoen for materielle- og personskader i tillegg til tap av menneskeliv reduseres eller ideelt sett unngås.

Dette prosjektet, som finner sted i Orkdal (sørvest for Trondheim), fokuserer på å undersøke effektiviteten av en geofysisk metode kalt elektrisk resistivitetstomografi (ERT) for kartlegging av slike områder. Dette er et samarbeidsprosjekt mellom Norges geologiske undersøkelse (NGU), Norges vassdrags- og energidirektorat (NVE) og Norges teknisk-naturvitenskapelige universitet (NTNU).

ERT innebærer å injisere strøm i bakken gjennom elektroder plassert i jorden. Disse elektrodene fanger opp resistivitetsmålinger fra bakken, som deretter brukes til å generere et todimensjonalt kart over undergrunnen basert på resistivitetsverdiene. Det er viktig å merke seg at denne kartleggingsteknikken utelukkende baserer seg på resistivitetsmålinger og ikke tar hensyn til andre faktorer knyttet til lagdeling i grunnen.

Ved å kombinere disse geofysiske målingene med ulike geotekniske undersøkelser, var det mulig å sammenligne hvilket detaljnivå som ble gitt av de geofysiske resultatene. Den geofysiske kartleggingen, basert kun på resistivitetsverdier, klarte å identifiserte plasseringen av sensitive områder.

Selv om det ble observert at ikke alle områder som ble markert som potensielt sensitive av de geofysiske resultatene faktisk viste seg å være det, var det et faktum at de faktiske sensitive områdene ble korrekt identifisert av den geofysiske metoden. Dette antyder at geofysisk kartlegging, som ERT, har potensialet til å effektivt avgrense mulig farlige områder.

Resultatene fra dette prosjektet gir støttende bevis for muligheten av å utnytte geofysiske kartleggingsteknikker for å identifisere og avgrense farlige områder, og dermed bidra til forbedret risikovurdering for, og tiltak mot, skredfare.

Contents

List of Figures

List of Tables

List of Symbols and Abbreviations

Symbols

U voltage [V]

R resistance [Ω]

I current [A]

S_u undrained shear strength [kPa]

c constant [-]

g acceleration of gravity [m/s^2]

m mass [g]

i average cone penetration [mm]

ρ resistivity [Ωm]

L length [m]

A area [m^2]

I_P plasticity index [%]

I_L liquidity index [%]

w_L liquid limit [%]

w_P plastic limit [%]

w water content [%]

B_q pore pressure ratio[-]

F_r normalized friction ratio [%]

Q_t normalized tip resistance [-]

S_r remoulded shear strength [kPa]

S_t sensitivity [-]

P_f vertical load [kg]

$\sigma_1 f$ [kPa]

γ unit weight [kN/m^3]

Abbreviations

ERT Electrical Resistivity Tomography

GPR Ground penetrating radar

HEM Helicopter Borne Electromagnetics

NGU Norway's national geological survey

NTNU Norwegian University of Science and Technology

NVE The Norwegian Water Resources and Energy Directorate

RCPTU Resistivity Cone Penetrometer Test

1 Introduction

This master thesis is a continuation of the in depth project completed in the fall of 2022. The project discussed both geophysical and geotechnical tests and their applicability in determining the presence of quick clay. The project presented mostly geophysical results from the project area, Orkdal valley. The geophysical results were from Helicopter borne electromagnetics (HEM), Electrical Resistivity Tomography (ERT) and refraction seismic tests. The geophysical results utilized further in this thesis is Electrical Resistivity Tomography (ERT). The project area, where the geophysical tests were completed, did not have any geotechnical data in the immediate vicinity. The geotechnical tests, such as drillings and lab tests were completed during the spring of 2023 and are presented in this master thesis. The location of both the geophysical and the geotchnical tests are presented in figure 5.

The idea is to determine in what capacity the geophysical tests can be utilized in mapping of potential hazardous areas. The potential is checked using geotechnical tests after the completion of geophysical mapping. If the geophysical methods used in fact can be utilized in order to narrow down the potential hazardous area, and therefore minimizing the needed geotechnical investigations, it can be both cost and time efficient. Reducing the time needed as well as the cost will enable quicker and more comprehensive tests at the most critical areas while eliminating, to some extent, the usage of time and money at not critical or hazardous areas.

This thesis will elaborate on how the geophysical and geotechnical methods correlate, and to which detail they do. This can be summarized as three research objectives for this thesis:

- Can ERT be used in order to accurately map hazardous areas?
- To what detail can ERT determine the soil layering?
- How well does ERT correlate with geotechnical tests?

1.1 Structure of the thesis

This thesis consists of 9 chapters structured the following way:

Chapter 1 is an introduction to the study performed in this master thesis, containing information on what has previously been completed as well as what is to be completed and its objectives.

Chapter 2 is briefly explaining details about the methods utilized in this study.

Chapter 3 is presenting a short overview of the most relevant theory used in this project.

Chapter 4 gives an overview of the fieldwork already completed before the start of this thesis, as well explaining the fieldwork conducted this spring.

Chapter 5 presents the samples examined in the laboratory.

Chapter 6 is presenting results, both the previously completed ERT and the new results from geotechnical field and laboratory work.

Chapter 7 is a discussion of the results together and what they indicate.

Chapter 8 is the conclusion of this thesis.

Chapter 9 has recommendations for further work in connection with this study.

2 Method

Before presenting detailed results and information about the project and its findings, the method for obtaining this information is presented. The method chapter is briefly elucidating how some results were obtained and handled as well as showing the setup for one important lab test. It also explains in short how precautions were made before commencing laboratory work.

2.1 Extracting pore water

There are different methods in order to extract pore water from a sample. The first method used in this project was not successful on the given samples and didn't produce any pore water for testing. This method utilized a chamber containing a test sample and a water filter. The chamber was connected to an air vent, which blew air at the sample inside the container. The idea is that the pressure from the air will blow the pore water out of the sample, through the filter, and then gathered in a cup for testing.

Another method is using a centrifuging device. An equal amount of soil sample is placed in four vials and are inserted into the apparatus. The apparatus will not start if the weight of the different containers are not equal, allowing a few grams of wiggle room. The machine will then over the course of 10 minutes spin the containers, compacting the material and pressing the pore water to the surface. This machine is seen below, and an example of how the pore water is collected at the surface is seen in figure 10. The setup for this method is shown in figure 1 below.

Figure 1: Pore water extraction using centrifugation device

2.2 Resistivity test

The other resistivity test than the one utilizing the pore water, measures the resistance of the soil directly. The test is set up as seen in figure 2. An amperemeter is connected to a power source and one side of the sample. The power source is connected to the other side of the sample. The voltmeter is attached with two wired needles which are inserted into the sample 50mm apart. A current is passed through the soil and using the readings from all devices, the resistivity can be calculated.

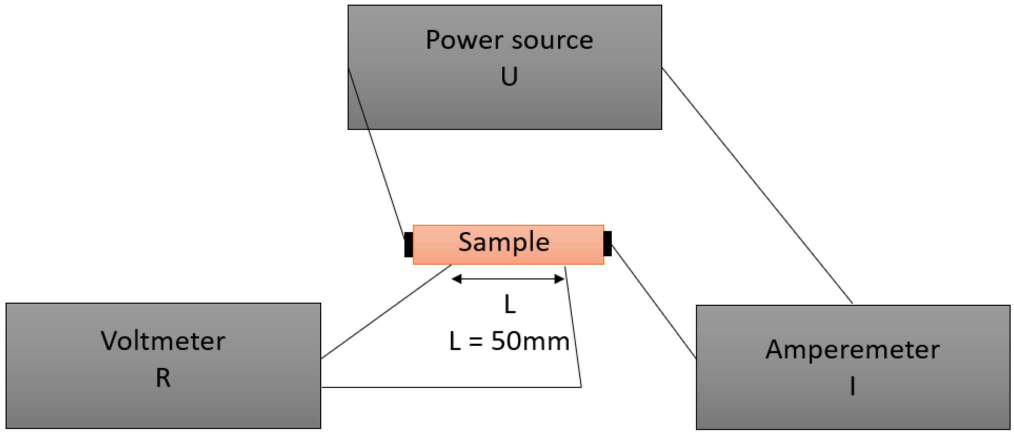

Figure 2: Resistivity test illustration

2.3 Lab tests

The method on how to perform the different lab tests are not elucidated further than some basic explanation provided in chapter 3 in conjunction with the theory around the specific tests. This because the execution of the tests are regarded as common knowledge for the intended readers of this thesis. The methods are all completed as instructed and explained in their respective standards.

2.4 Field results

Results from drilling were read into Trimble Novapoint GeoSuite Toolbox 16 and then further extracted to AutoCAD in order to get the visual plot. For the RCPTU, Statens Vegvesen has an excel-tool in which you can input your data and get graphs as well as interpretation of the layering. This excel-sheet was used in this study, the version used was v.2023.02(Statens Vegvesen 2023). Versions of AutoCAD used is 2020 and 2023.

3 Theory

3.1 Lab tests

Lab tests are used in order to classify a material and getting its properties. The main objective is to prove or disprove the presence of quick clay, and therefore the tests described will be selected because of their direct connection to helping prove or disprove this.

3.1.1 Fall cone

The fall cone test is a common geotechnical test used to measure the consistency of soil. This test is particularly useful in determining the shear strength of soft and sensitive soils such as quick clay. Quick clay is a type of clay that exhibits a high sensitivity to changes in stress and strain, making it prone to sudden and catastrophic failures.

The fall cone test involves dropping a cone-shaped device with a standardized weight onto the surface of the soil. The cone is allowed to penetrate the soil for a short time interval, and the depth of penetration is recorded. The test is repeated several times, typically three, and the results are noted.

The fall cone test is essential in proving the presence of quick clay. The definition of quick clay is having a remoulded shear strength less than $0.5kN$. (NGF 1982)

The shear strength both for undrained and remoulded fall cone test is calculated with the equation seen below.

$$Su = c \times g \times m/i^2 \tag{1}$$

- c: constant, dependent on the tip angle of the cone
  - $c = 0.8$ for 30 degree tip angle
  - $c = 0.27$ for 60 degree tip angle
- g: acceleration of gravity, set at 9.81 m/s^2
- m: mass of the cone
- i: average cone penetration

(Standard Norge 2017)

3.1.2 Resistivity from resistace test in lab

Following are the equations used in order to calculate resistivity using the equipment in the lab. The first equation presented is Ohm's law which explains the relationship between voltage, current and resistance. Using a uniform conductor with known length and cross-sectional area allows for the second equation describing the resistance using resistivity and these known values. Rearranging the second formula gives the third, and finally the Ohm's law is substituted in for R.

$$U = R \times I \quad \text{(Ohm's law)} \tag{2}$$

$$R = \rho \times L/A \tag{3}$$

$$\rho = \frac{R \times A}{L} = \frac{U}{I} \times \frac{A}{L} \quad [\Omega m] \tag{4}$$

where:

- U: voltage
- R: resistance
- I: current
- ρ: resistivity
- A: cross-sectional area
- L: length

(Svoboda and Dorf 2014)

3.1.3 Water content

Water content is determined by measuring the weight of a sample specimen before and after drying it in an oven. This calculation involves comparing the difference in weight to determine the amount of water present. The water content is known to exhibit a correlation with the mechanical properties of materials, making it an essential index parameter. The following formula demonstrates the calculation of water content using the mass of water and the mass of the dry specimen.

$$\begin{gathered} \text{water content} = \frac{m_w}{m_s} \times 100 \quad [\%] \\ \text{Where } m_w = m - m_s \end{gathered} \tag{5}$$

- m_w: mass of water [g]
- m_s: mass of solids [g]

- m: total mass before drying [g]

(Standard Norge 2014)

3.1.4 Atterberg limits (liquid and plastic limit)

The Atterberg tests are a series of laboratory tests used in geotechnical engineering to determine the physical properties of soil. It involves manipulating remoulded test samples. The tests are used to identify the liquid and plastic limits of a soil sample, which are important indicators of its behavior under different moisture conditions. Liquid limit and plastic limit are two of the Atterberg limits for soils. The liquid limit of a soil refers to the water content at which the soil transitions from a liquid to a plastic state. This can be determined by two methods, where one is the Casagrande method.

The plastic limit of a soil is the water content at which the soil is no longer plastic when subjected to further drying. (Standard Norge 2018a)

3.1.5 Liquidity index and plasticity index

With the liquid and plastic limit known, the liquidity and plasticity indexes can be found using the following formulas. The liquidity index characterizes the correlation between the moisture content and the plasticity range of a soil. The plasticity index is used for classification of plastic soils depending on their plasticity value. (NTNU 2017)

$$I_P = w_L - w_P \tag{6}$$

$$I_L = \frac{w - w_P}{w_L - w_P} \tag{7}$$

where:

- w_L: liquid limit [%]
- w_P: plastic limit [%]
- w: water content [%]

(Standard Norge 2018a)

3.1.6 Uniaxial test

The uniaxial test is a laboratory test used in geotechnical engineering to determine the strength and stiffness of soil samples. The test is used to measure the response of soil under stress and strain conditions.

The uniaxial test applies a single axial load to the soil sample, which is typically cylindrical in shape. The test measures the deformation and strength of the soil under axial compression. The results of the uniaxial test are used to determine the compression strength and stiffness of the soil.

(Standard Norge 2018b)

3.1.7 Grain size distribution

Grain size distribution analysis is a crucial component of geotechnical lab work, specifically in the study of soil and sediment samples. It involves sieving the sample through a series of different-sized sieves to determine the proportion of various grain sizes present. By weighing the retained material on each sieve and calculating cumulative weight percentages, a grain size distribution curve is constructed. This curve provides valuable insights into the sample's composition, including the percentages of gravel, sand, silt, and clay. (Statens Vegvesen 2022)

3.2 RCPTU

The Resistivity Cone Penetrometer Test (RCPTU) is a commonly used drilling method in geotechnical engineering. By driving a cone-shaped penetrometer into the ground at a controlled rate and depth, the RCPTU test provides valuable data on resistance to penetration, pore water pressure and the electrical resistivity of the soil at different depths.

It assists in evaluating factors like foundation bearing capacity and lateral earth pressure on retaining walls. One of its key advantages is the ability to measure pore water pressure. This factor is critical as it affects the stability of soils and slopes. (Solberg et al. 2016) (Pfaffhuber, Bazin, and Helle 2014) (Pfaffhuber et al. 2016)

3.3 Electrical resistivity

Electrical resistivity in the ground refers to the property of soil and rocks that hinders the flow of electric current beneath the Earth's surface. It is the inverse of electrical conductivity. The resistivity value is influenced by factors such as the composition of the soil and the moisture content present. Soils and rocks with higher water content exhibit lower resistivity due to water's conductive nature, facilitating electric current flow. Conversely, drier soils and rocks display higher resistivity since the presence of water is necessary for efficient current conduction. The conductivity of water is also influenced by its salt content, as salts contribute to its electrical conductivity. Additionally, the type of material in the soil impacts its resistivity. Soil and rocks with elevated clay content exhibit higher resistivity compared to those with a greater proportion of sand. This distinction arises from the denser packing of clay particles, which restricts the flow of electric current through the material.

The measurement of ground resistivity can be accomplished through various techniques, such as Electrical Resistivity Tomography (ERT) and Helicopter Borne Electromagnetics (HEM). These methods allow for the mapping and visualization of subsurface resistivity variations, aiding in the characterization of geological formations, groundwater exploration, and environmental assessments. The expected resistivity values for some materials are shown below.

Table 1: Expected soil types based on resistivity (Solberg et al. 2012) (Solberg et al. 2008) (Noon, Stickley, and Longstaff 1998) (Long et al. 2012)

Material	**Resistivity [Ωm]**
Marine clay	1-10
Leached clay	10-100
Silty material	50-150
Sand, gravel	>150
Bedrock	1 000-10 000

The leached clay area from 10-100 is not the only rage where there has been found quick clay. Rømoen found quick clay in the range 5-90, so the range might be a bit fluid and dependant on the specific soil. (Rømoen et al. 2010)

In geological contexts, the transition from one layer to another is often characterized by a smooth gradient. Consequently, determining the precise depth of layers, particularly the bedrock, may lack accuracy due to diminishing precision as depth increases. Moreover, the materials constituting these layers frequently exhibit properties that result in gradual transitions rather than distinct boundaries between them. (Pfaffhuber, Bazin, and Helle 2014) (Solberg et al. 2016)

3.4 Electrical resistivity tomography (ERT)

Electrical Resistivity Tomography (ERT) is a geophysical method that utilizes electrical current to quantify the resistivity of subsurface materials. This technique involves injecting a small electric current into the ground and measuring the resulting electrical resistance at various points on the surface.

ERT employs a series of electrodes placed at regular intervals on the ground surface. A controlled electric current is passed between two electrodes, and the voltage at each electrode is measured. This voltage is again calculated into resistivity. The collected data is then utilized to construct a two-dimensional representation of subsurface electrical resistivity.(Long et al. 2018) (NGI 2023)

Different subsurface materials exhibit distinct electrical resistance, enabling differentiation when measured at the surface. The electrical resistivity values of subsurface materials offer valuable insights into their composition and structure. Varied materials, including rocks, soils, and groundwater, exhibit unique electrical resistivities. Patterns of electrical resistivity observed in the subsurface can thus aid in identifying the presence and spatial distribution of these materials.

A notable advantage of ERT is its capability to provide detailed subsurface mapping. By employing a dense array of electrodes and measuring electrical resistivity at multiple surface points, ERT can generate high-resolution images that reveal the distribution and extent of different subsurface materials. Such information proves instrumental in understanding site geology and anticipating the presence of specific materials.

ERT demonstrates versatility as it can be applied across diverse environments, ranging from urban areas to remote wilderness, and can be employed for various subsurface materials, including soils, rocks, and groundwater.

However, ERT also entails certain limitations. Primarily, this method solely provides information regarding subsurface electrical resistivity, which may not necessarily correspond to the composition or physical properties of the subsurface materials. For instance, two different types of rock may possess identical electrical resistivity but exhibit contrasting mechanical properties such as strength or permeability.(Pfaffhuber et al. 2016) (Bazin and Pfaffhuber 2013) (With et al. 2022)

4 Fieldwork

Careful planning is important before completing work in the field for several reasons. Insufficient planning may lead to delays or extra work needing to be done which increases costs. It is also important in order to get the most valuable information from the project area. In geotechical drilling, it is important that the drilling site has a good availability, in order for the drilling rig to be able to access and operate. This particular challenge was thought to be solved in our case by the drill operator visiting the different planned sites after the initial drilling plan is made, however one of the drill sites turned out to be unreachable with the rig. This is explained in further detail later.

A drilling plan was made on the basis of the ERT results. The responsible personnel for this project at NGU made a preliminary suggestion of a drilling plan and presented it to the others involved. After positive feedback on the selected drilling areas and selected tests as well as an agreement between NTNU and NGU on the distribution of costs they would cover, a final plan was created. The changes from the preliminary plan to the final plan was focused around how much the project could afford to spend on the different areas. The final plan is presented in figure 3. Some elements in the drilling plan was still undetermined before the drilling was in progress. The reason for this being that some points were dependant on the findings from total sounding/RCPTU such as whether or not to take a sample from the ground and at what depth.

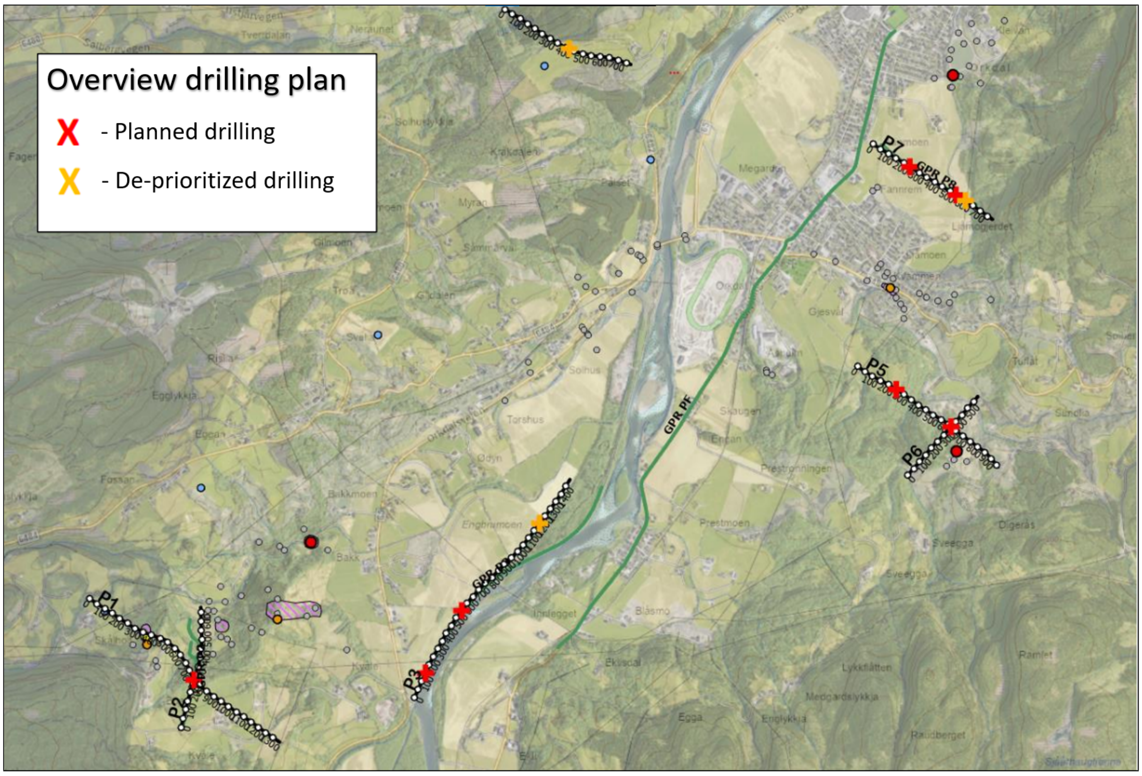

Figure 3: Drilling plan

In the figure above, it is shown how the boreholes location correlate with the location of the ERT profiles. The green line indicates a previously completed GPR measurement. The yellow crosses indicated de-prioritized drilling spots as shown. These were initially planned drill locations, but were de-prioritized in order to keep the project's budget.

A preliminary idea of where to take samples were based on the ERT results, however the total sounding/RCPTU gives the exact strength parameters of the drilling location, and gives a more detailed view of where it is most appropriate to take a sample and at which depths.

4.1 Drilling

After the budget was clear as well as the drilling plan, the drillings started 09.03.23 in P7. Both $P7_1$ and $P7_2$ were drilled this day. The total sounding were completed without any problems. There was an aim to do a RCPTU drilling as well as sampling from $P7_2$, however the ground conditions were to hard for the RCPTU to penetrate. Given the stiff soil conditions, the plan for taking a sample was discarded here. Further the drilling for $P5_1$ was put on hold because of the boring rig's inability to access the site due to the large amount of snow. The drillings $P3_1$ and $P3_2$ was therefore prioritized first. The drilling at the intersection between P1 and P2 followed. The drilling location had to be moved slightly because of the steep inclination at the exact point. Figure 4 shows the light blue indicating the planned drilling location and the green spot being the new location. $P5_1$ was drilled without complications when the weather conditions allowed it. Figure 5 shows the location of all drillings as well as the ERT-lines. The figure was made with specific coordinates after all drillings were completed. At point P_1P_2 and $P5_1$ there was also completed RCPTU at the same spot as the shown total soundings.

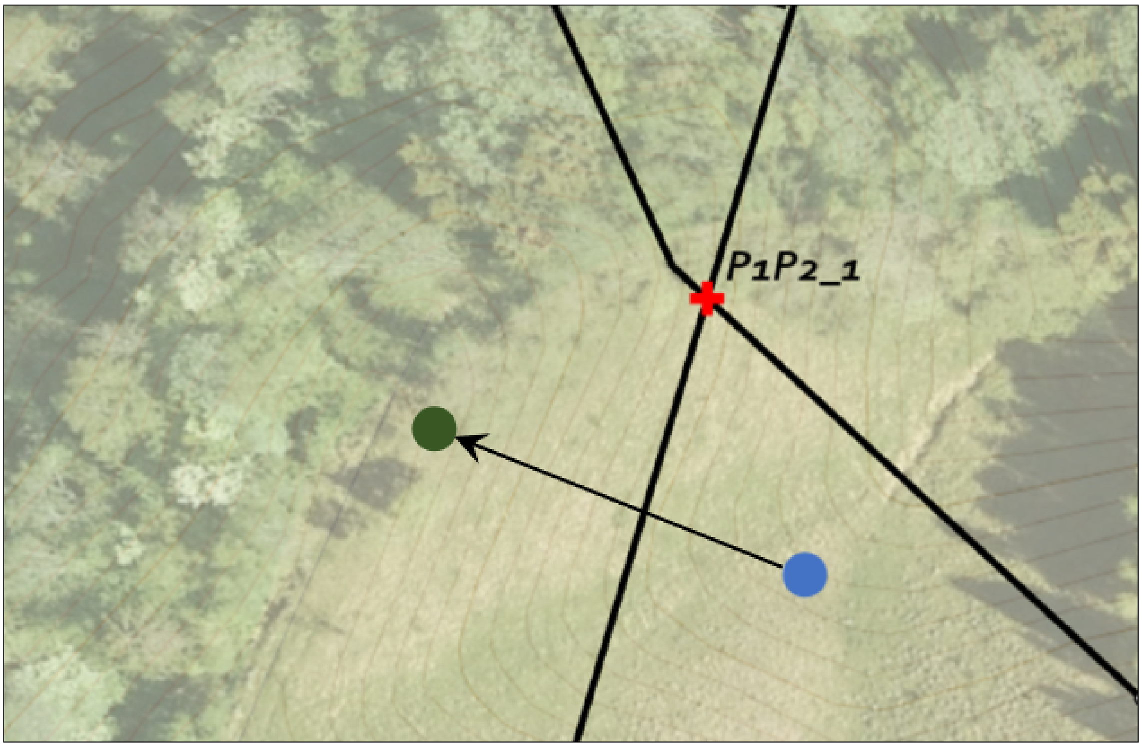

Figure 4: Relocation of drilling between P1 and P2

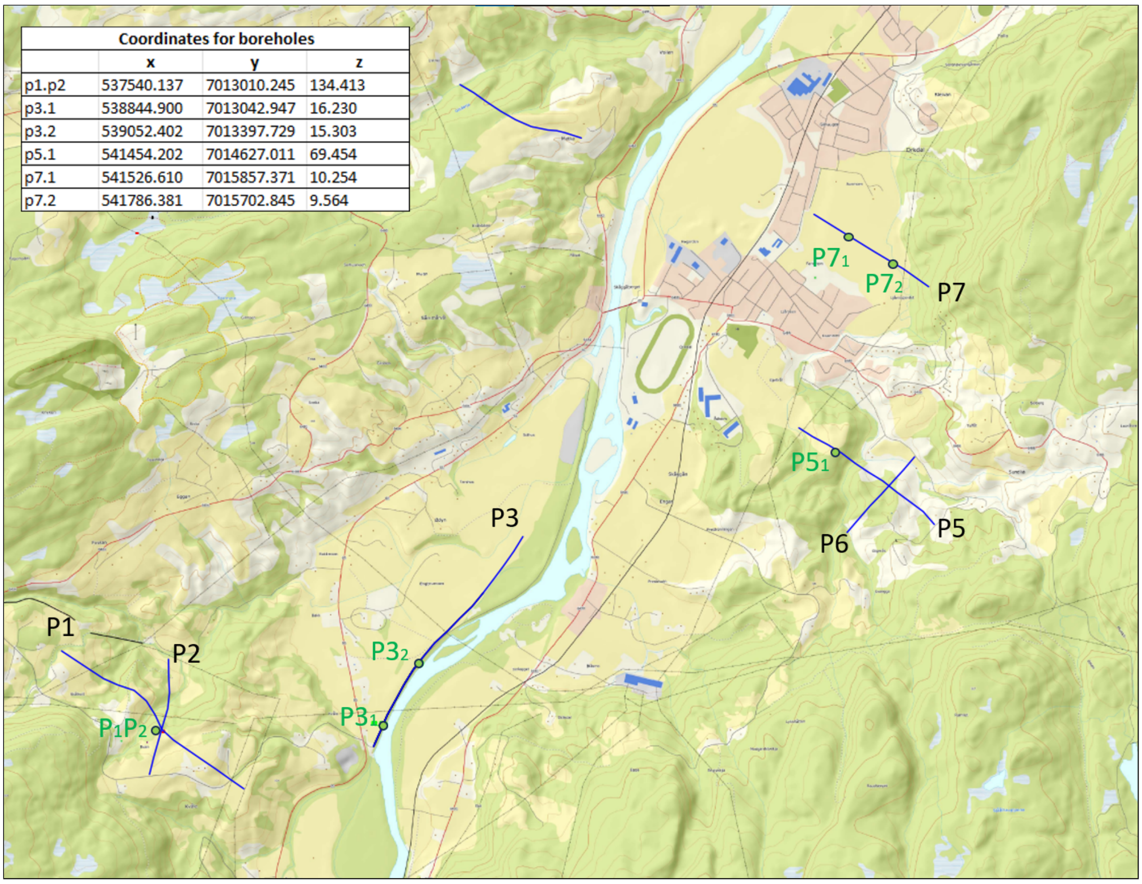

Coordinates for boreholes			
	x	y	z
p1.p2	537540.137	7013010.245	134.413
p3.1	538844.900	7013042.947	16.230
p3.2	539052.402	7013397.729	15.303
p5.1	541454.202	7014627.011	69.454
p7.1	541526.610	7015857.371	10.254
p7.2	541786.381	7015702.845	9.564

Figure 5: Final drillplan with ERT-lines

4.2 Limitations

There are some limitations in this study because of the lack of diverse results. Several field investigations and tests were discarded for different reasons. At the $P7_2$ borehole, it was supposed to be carried out RCPTU as well as sampling. Both the RCPTU and the sampling was scrapped because of the hard ground conditions. The RCPTU was unable to penetrate the ground, and since the RCPTU was to be used as basis for sampling spot, as well as the hard soil conditions, it was scrapped all together. At the intersecting ERT-lines 5 and 6 there was also supposed to be RCPTU and sampling, as well as total sounding. The rig was unable to reach the site because of a bridge possibly not having the capacity to withstand the weight of the rig. It was considered to drive the rig through a river nearby instead of over the bridge to reach the site, but the water flow made this impossible.

5 Labwork

Before commencing the labwork, the preparations are important. Both for the best possible execution of the tests, as well as being able to do them as quickly as possible. Doing them quickly is necessary in order for the sample to dry out as little as possible. Drying out will change the actual water content of the sample and may give incorrect results. This is also the reason why properly packing the portions of the sample which are not tested right away is essential.

A template of how the sample is planned to be divided into pieces is also a good thing to have. This way it is clear which parts of the sample are to be used for which test. This will only work as a help and is not absolute. The condition of the sample can not be predicted and needs to be looked at in the lab after extraction. It then has to be decided if the model can be applied or not. Some of the tests require better sample quality than others and are more sensitive to disturbances. These sensitive tests are for example oedometer test and fall cone. Tests more suitable to the places with disturbance on the sample is for example water content.

In coordination with NGU and NVE, it was decided to complete the following tests for the samples:

- Water content x 3
- Grain size distribution
- Fall cone
- Density ring
- Plastic limit
- Liquid limit
- Oedometer [1]
- Salinity/Resistivity
- Resistance test

They are all completed in accordance with the procedure specified in their standards as well as Statens Vegvesens handbook V220. (Statens Vegvesen 2022)

Some of the tests were not completed for some samples for different reasons, and the reason is explained in more detail under the sample/limitation section. An overview of where the different test were completed on each sample is seen in Appendix D.

[1] The results of the oedometer tests were compromized as some of tests got cracks/disturbances when mounting into the device and were therefore chosen to not include

5.1 Sources of error

All work completed have sources of error to some degree, and the labwork completed is no exception. Due to the fact that several of the tests are dependant on readings done by eye, for example reading results of a graph, the result derived may deviate slightly from the actual result itself.

5.2 Health, safety and environment, HSE

Before starting to work in the laboratory, it is important to consider any risks that may cause harm to people or equipment. A course from NTNU outlining the risks of completing labwork and precautions to take when doing this was completed. A thorough walk through of the lab and its equipment was also completed with personnel employed at NTNU. This in order to have the necessary prerequisites for completing the lab work in a safe way. When this was in order the samples were extruded and tested.

5.3 Samples

All samples are from borehole P_1P_2. They are 54mm in diameter and 74cm in length.

5.4 Sample 1

This is the first sample extracted from borehole P_1P_2 (3-4m depth). The high resistance seen from the total sounding was the reason for this sample to be taken, since it was deemed important to see what masses was present here. Pictures of the extruded sample can be seen under in figure 6. It was extremely hard and difficult to cut through. The sample cracked near the top while extruding the sample.

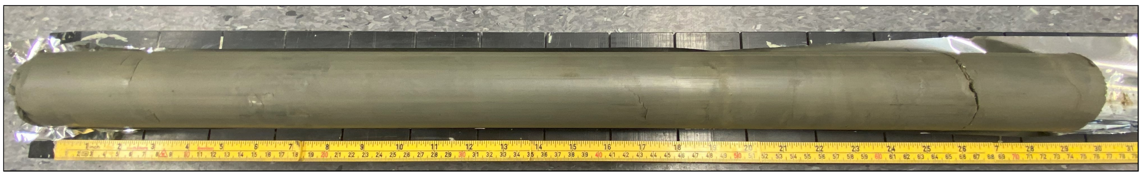

Figure 6: Sample 1

The crack forming under extrusion may be caused by a weak layer within the sample with a low binding effect. This hypothesis is strengthened by the visual appearance of seemingly dry sand particles and layers within the sample when cut. Below is an example of where the sand is seen within the sample as well as a small rock.

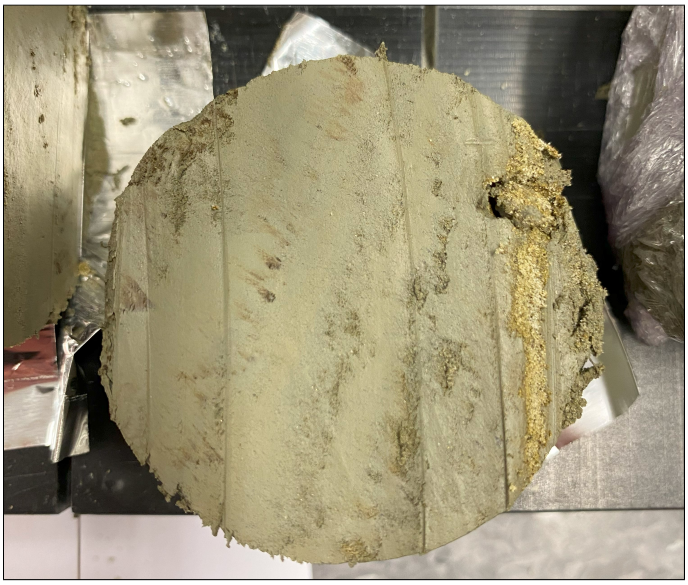

Figure 7: Visible sand and rock in sample 1

This sand can create weak areas within the sample and may cause the soil to crumble when exposed to stress in certain directions. It was not possible to extract pore water from this sample using the methods described under method, so the salinity test was dropped.

5.5 Sample 2

Sample number 2 (9-10m depth) was a much softer sample than sample 1. It still didn't look to be any form of sensitive clay. The visual appearance looked like firm intact silt/clay. It was more smooth to cut through when dividing the sample and gave no difficulties. There were however found small rocks in sample 2 as well as in sample 1.

Figure 8: Sample 2

Sample 2 was seemingly consisting of homogenous soil, with no visible layering throughout. It all had a grey/blue like color as shown in figure 9.

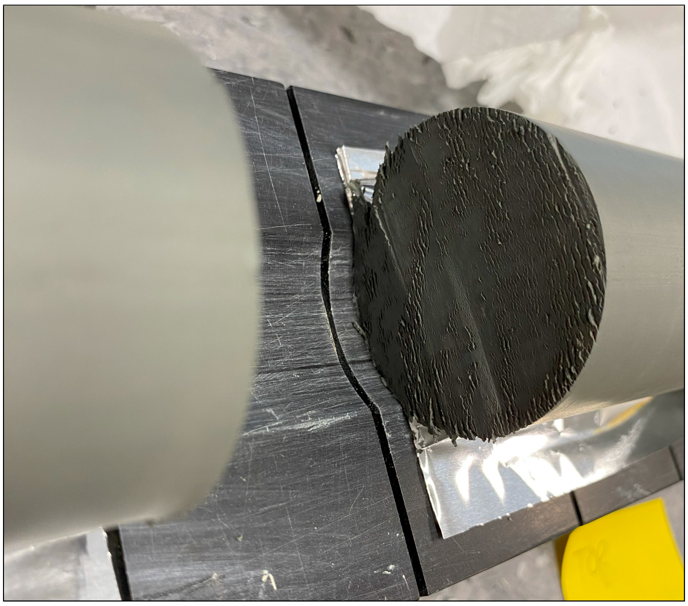

Figure 9: Sample 2 cross section

Since this sample was a lot wetter than the previous one, it was possible to extract pore water using the centrifugation apparatus. One of the vials containing water from sample two is seen below.

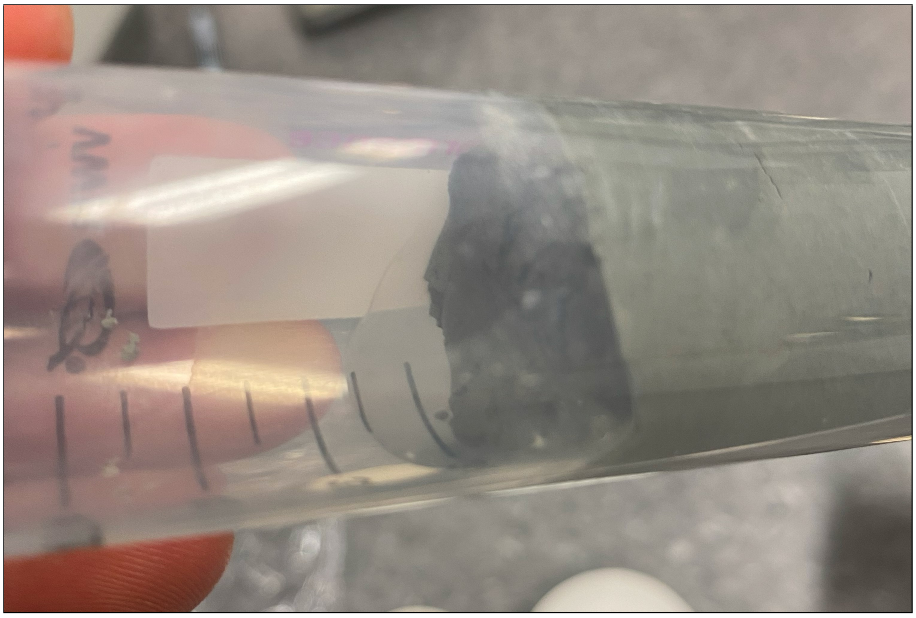

Figure 10: Pore water sample 2

5.6 Sample 3

Sample 3 (13-14m depth) was soft to cut through at the top but harder at the middle and bottom. At first glance it seemed a bit crumbly at bottom, giving an indication of the presence of sand or silt. There were no visible disturbances after the extrusion, but cracks appeared at some areas during the cutting of the sample. This is shown in figure 11, where cracks appeared close to where the sample was being cut through. This could be an indication of soil in the sample with a low binding effect, i.e sand. The areas with sand may be more inclined to crumble when the sample is put under a certain amount of stress when utilizing the cutting saw.

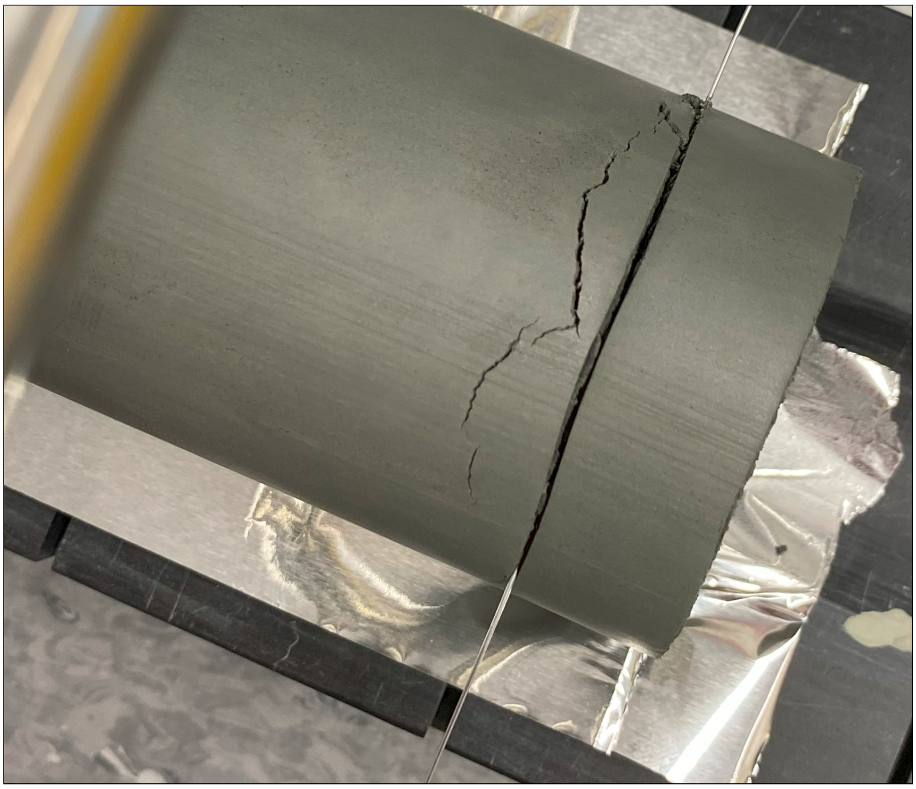

Figure 11: Cracks forming during cutting

5.7 Sample 4

Sample 4 (22-23 m depth) was a bit softer than the previous samples when cutting through. When extruding the sample it had no visible external disturbances with the exception that it cracked near the top. When dividing the sample, it had what looked like visible grains along some of surfaces, as seen in fig 13a below. It had a bit darker color near the top which is also shown below. This can be caused by some compression during extrusion, or it may just be how the soil was in situ.

(a)

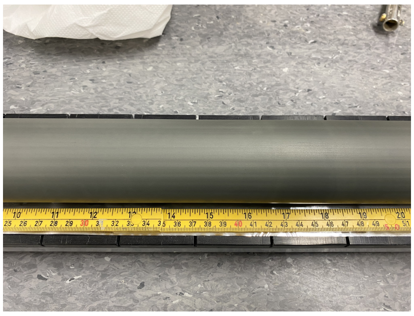

(b)

(c)

Figure 12: Sample 4

The soil was seen to be not entirely homogeneous when dividing. There are visible grains in 13a) while at 13b) the soil grains are not visible. In b) however it is clear that while cutting, the sample created horizontal cracks at the cutting surface. This indicates that the sample could be dry, or have other properties making it sensitive to relatively small disturbances in this direction. The visible grains seen in a) was at the surface where the sample cracked under extrusion.

(a) Grains visible near top sample 4

(b) Cracks while cutting near bottom sample 4

Figure 13: Sample 4 cutting surfaces

5.8 Sample 5

Sample 5 (40-41m depth) was suspected to contain quick clay, which was also indicated at extrusion. The sample was very soft to cut through, and got deformed at bottom during extrusion. The sample was visibly wet and had external disturbances along the sample.

Both the deformed bottom of the sample as well as the external disturbances is seen below. These deformations and disturbances made the usable sample areas for sensitive tests smaller. These areas were therefore as good as possible used for the tests not dependant on the soils condition.

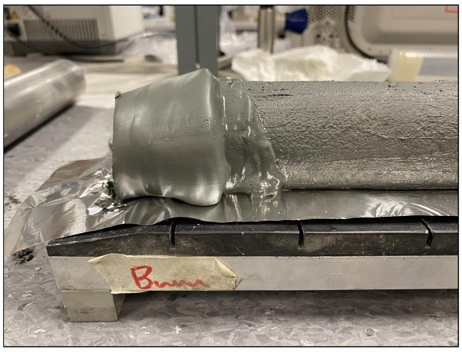

(a) Compressed bottom of sample 5

(b) External disturbance sample 5

Figure 14: Sample 5 disturbances

It was also noted that the inside of the sample was considerably wetter than the outside. Its strength also plummeted when remoulding the sample. It is shown below how a part of the sample is in three different stages. It looked to be somewhat stiff before cutting, but when cutting the sample open it was visibly very wet. When remoulding it instantly broke together and acted like a heavy liquid.

(a) Fall cone undisturbed

(b) Glistening inside cut

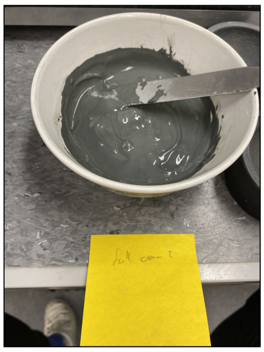

(c) Remoulded

Figure 15: Sample 5 undisturbed and remoulded

6 Results and discussion

For this project, there are direct results from both field- and labwork. The results are presented and briefly discussed continuously. Firstly the previous results, then the geotechnical field results and lastly the results from the laboratory. The results are discussed together in chapter 7.

6.1 Previous results, ERT and HEM

In the project area there are previously completed ERT and HEM results. The ERT results are to be compared with the following results from geotechnical drillings and labwork. The HEM results don't have the same detail as the ERTs have in order to compare with detailed results from field and lab. Given that the HEM has a larger interval between each measurement the resolution will have slightly lower density and accuracy. Still, the ERT was completed with 5m intervalls between each electrode and the results are interpolated between them. Meaning the ERT also contains some factor of inaccuracy in its measurements and resolution. The ERT profiles are presented below and are used for comparison in chapter 7.2. The ERT-profiles are also presented in a larger format in Appendix B. All profiles were obtained from NGU. (Larsen 2022)

The colors representing the different resistivity values are presented below.

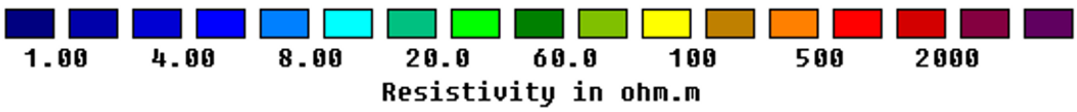

Figure 16: ERT color values

6.1.1 P1

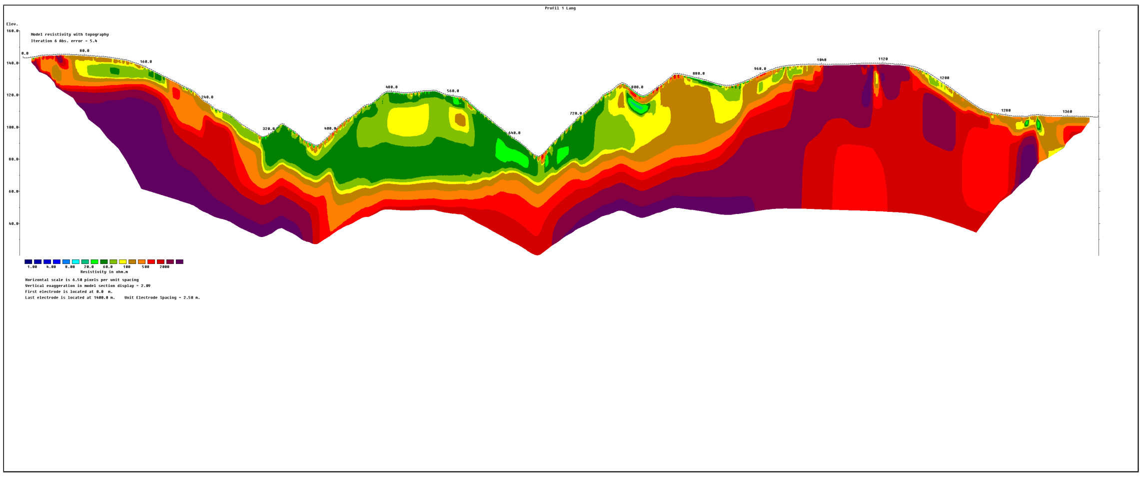

Figure 17: ERT P_1

6.1.2 P2

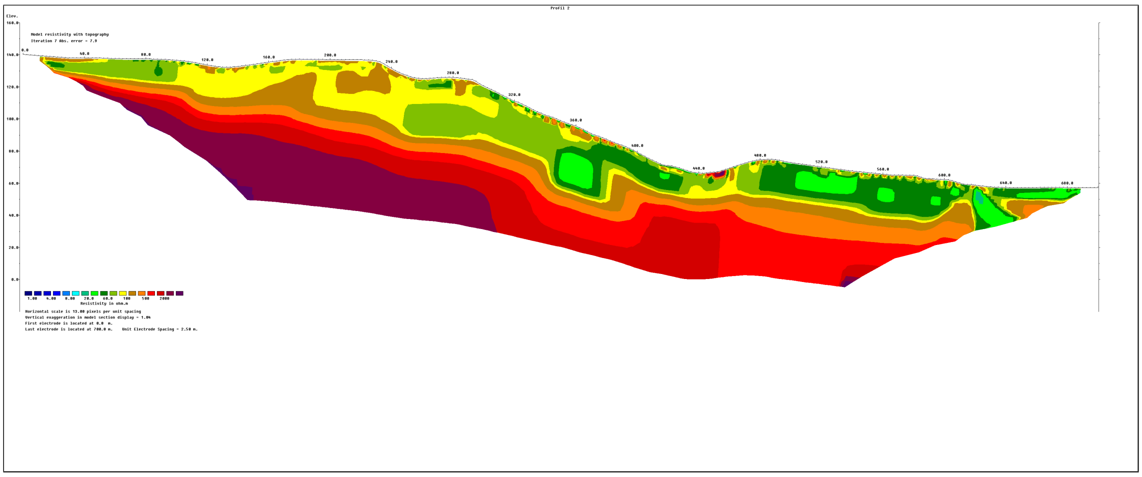

Figure 18: ERT P_2

6.1.3 P3

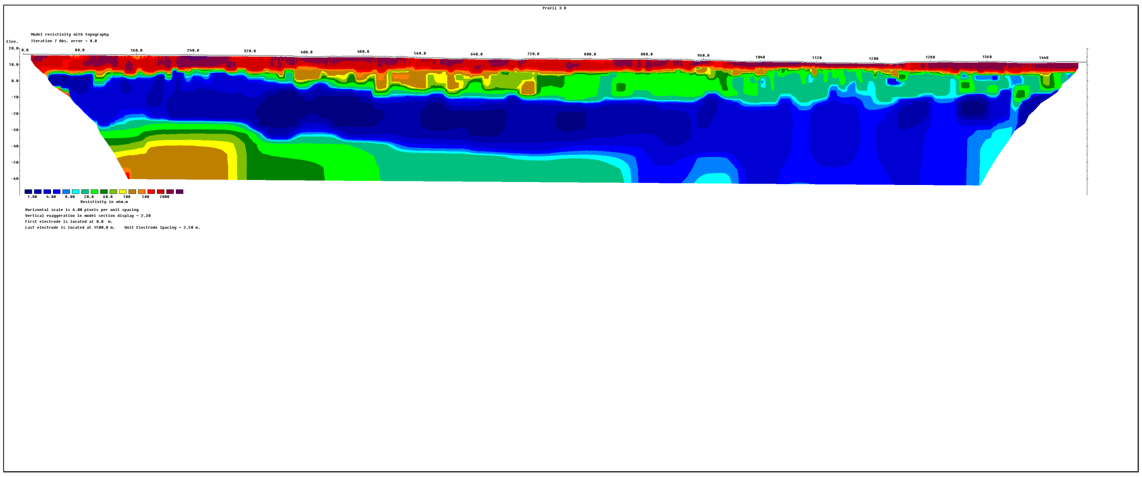

Figure 19: ERT P_3

6.1.4 P5

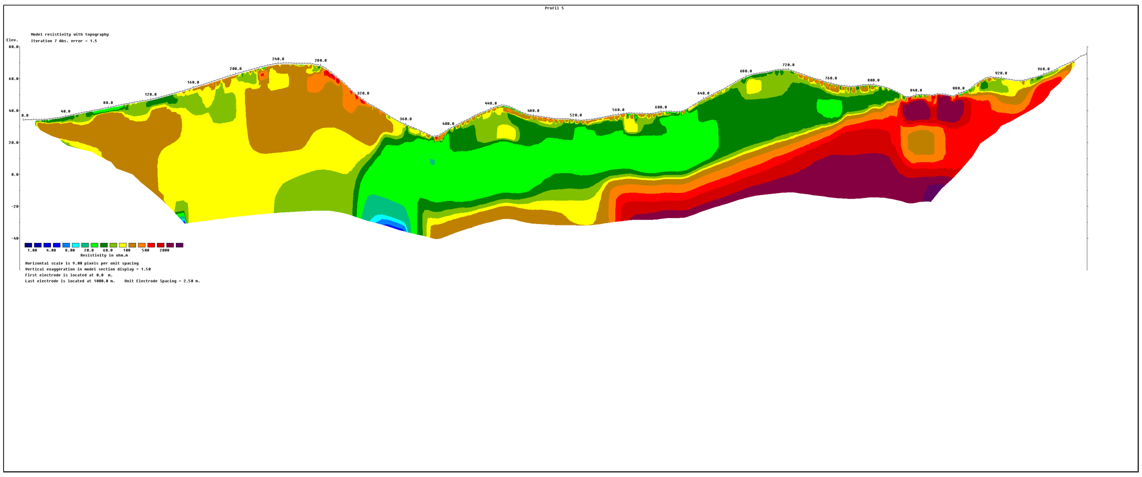

Figure 20: ERT $P5_1$

6.2 Results from geotechnical fieldwork

The results from all drillings, both total soundings and RCPTUs are shown below. They are shown in a larger format in Appendix C where each drilling has its own page. They are combined with the previously shown ERT data plots in the next chapter for interpretation.

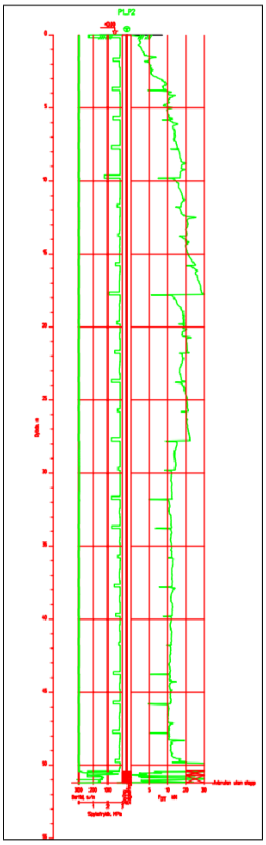

Figure 22: P_1P_2 total sounding

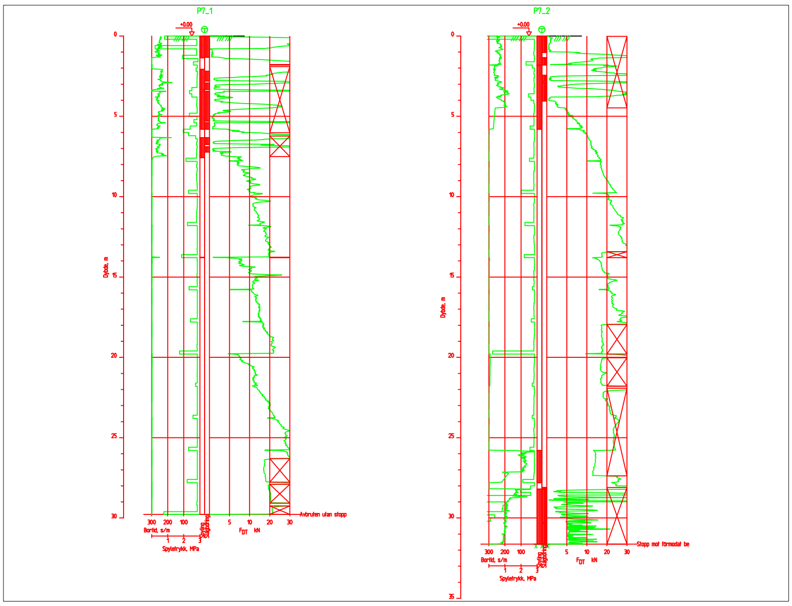

Figure 23: Total soundings $P7_1$ and $P7_2$

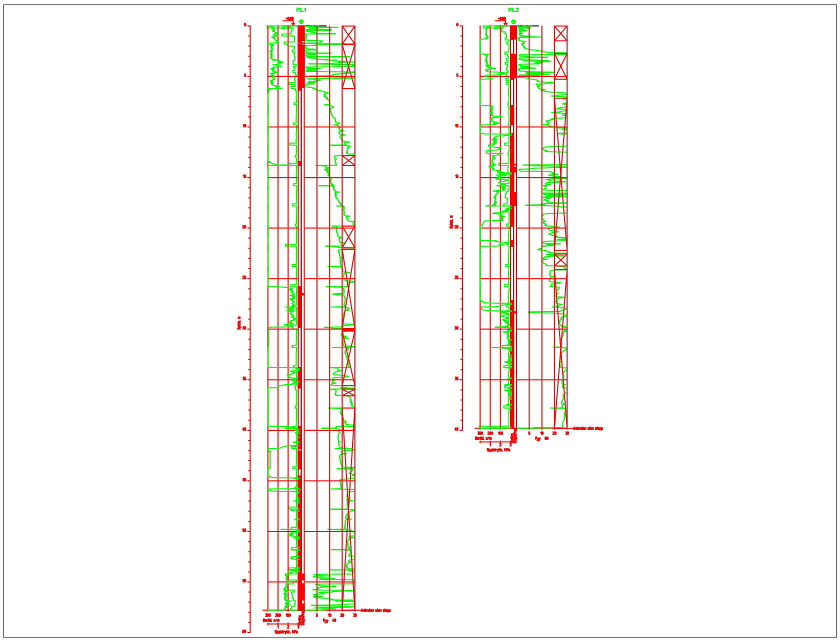

Figure 24: Total soundings $P3_1$ and $P3_2$

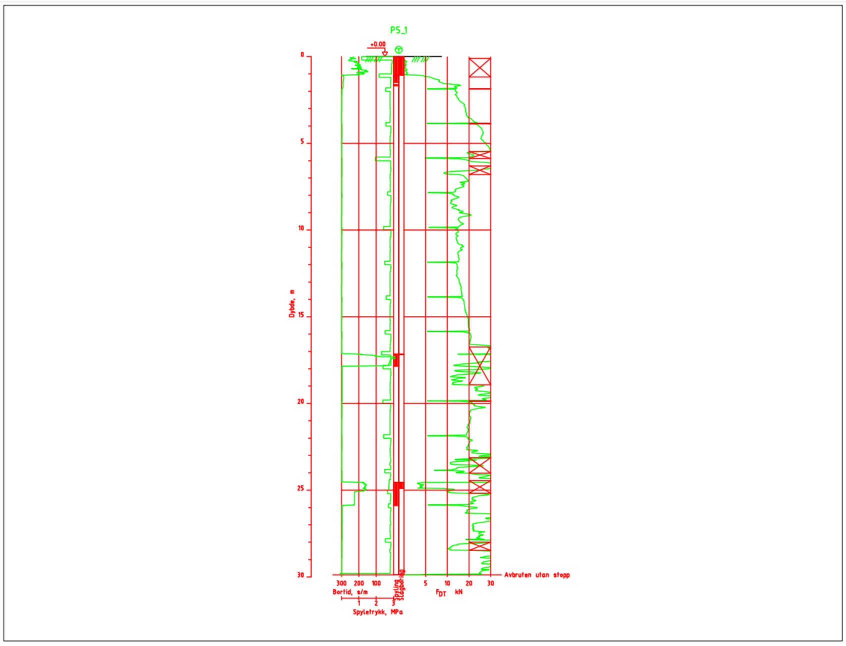

Figure 25: Total sounding $P5_1$

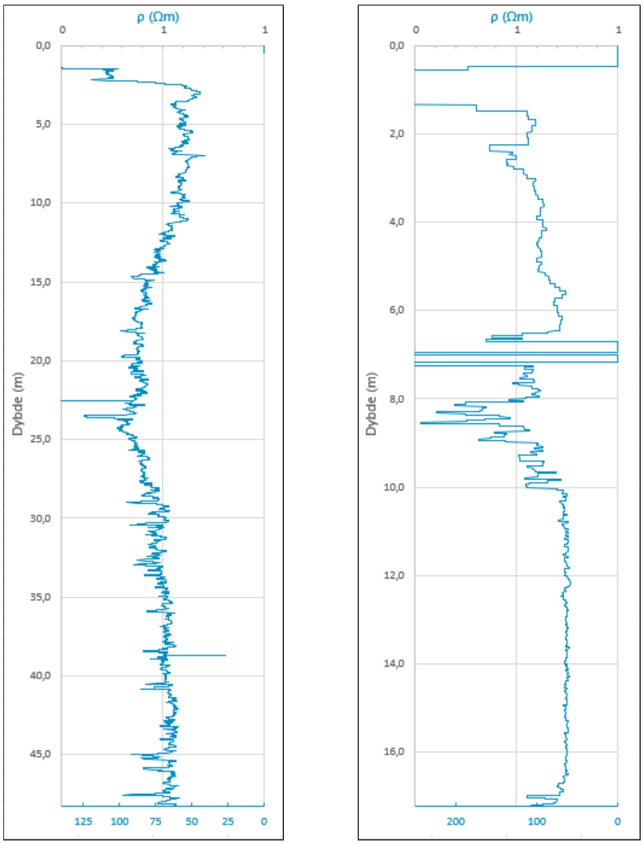

Figure 21: Resistivity from RCPTU P_1P_2 (left) and $P5_1$ (right)

When inserting the CPTU-files into the CPTU excel-sheet from Statens vegvesen, it is also possible to create a layering profile based on the file data seen below. Also inserting the calculated unit weight for the soil for different depths, increases the accuracy of the interpretation. This was done for both CPTUs and used as basis for interpretation seen in appendix Appendix A. Underneath is the resulting interpreted layering of the CPTU in P_1P_2. The figure uses B_q, F_r and Q_t which are listed with explanation below. They are all calculated automatically in the excel-sheet from Statens Vegvesen.

- B_q: Pore pressure ratio, calculated with pore pressure readings and tip resistance.
- F_r: Normalized friction ratio, calculated with side friction and tip resistance.
- Q_t: Normalized tip resistance, calculated with tip resistance and effective overburden pressure.

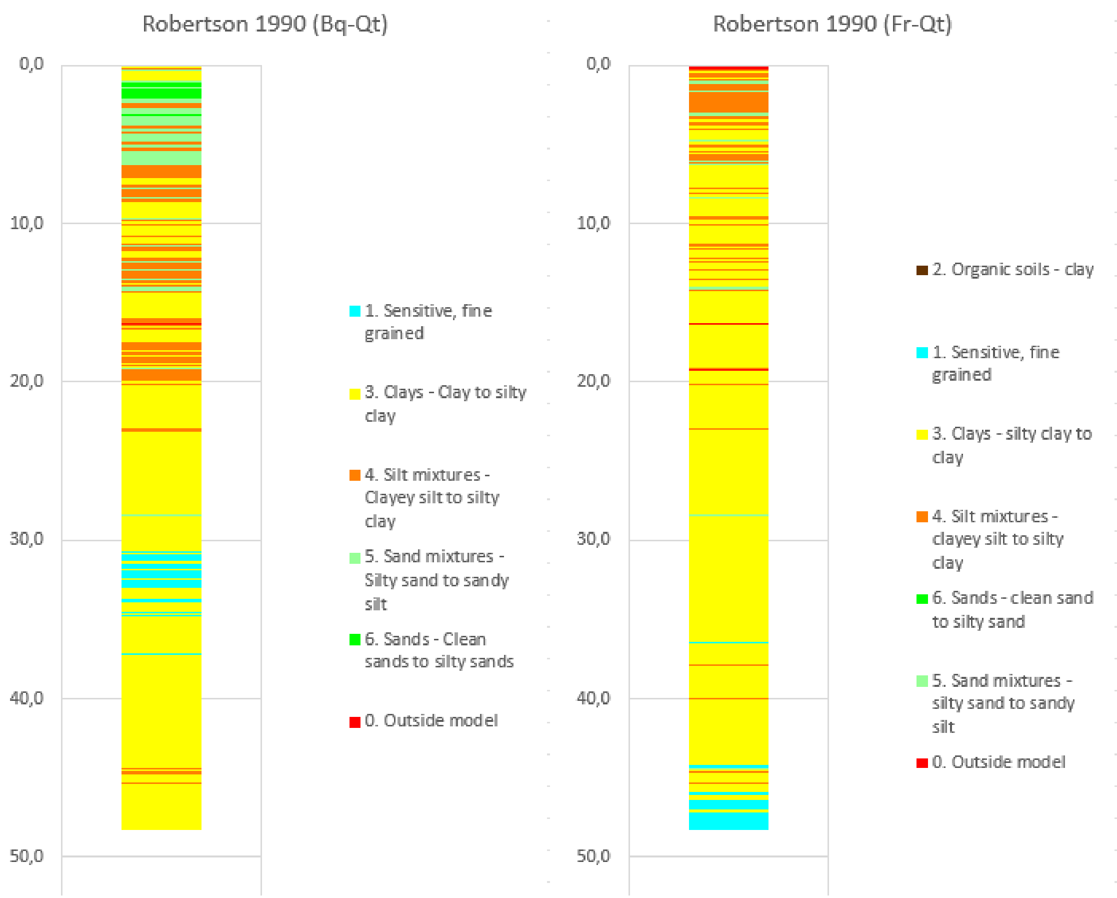

Figure 26: Layering based on RCPTU in P_1P_2 (Statens Vegvesen 2023)

The layering produced from Statens vegvesens excel-sheet coincides well with what was expected from ERT and total sounding. It also gives a good indication on what to expect from the extracted samples at the cite. The two methods have marginal differences with the largest one being that the Bq-Qt chart interprets a larger amount of silt in the clay (the orange areas) than the Fr-Qt chart. At the top of the charts they differ a bit with both charts having a lot of very thin layers, probably because of the roughness of the soil and the top soil itself containing a larger mixture of mechanical properties than the more homogeneous soil deeper into the ground. The differences at lower depths however is almost just over how sensitive or silty the clay is, they both agree on the dominant presence of clay. They also differ on where the largest presence of sensitive soil is found.

6.3 Results from labwork

6.3.1 Water content

Three water content tests were conducted for each sample. The three include one from the top, one from the middle and one from the bottom of the sample. They are listed from top to bottom of each sample in the table below.

Table 2: Water content

Sample no	Mass dry sample [g]	Mass water [g]	Water content
	18.8	4.8	25.53 %
1	19.5	5.2	26.67 %
	9.8	2.8	28.57 %
	33.8	9.4	27.81 %
2	24.9	6.9	27.71 %
	34.9	9.7	27.79 %
	25.8	7.1	27.52 %
3	33.7	9.2	27.30 %
	38.2	8.9	23.30 %
	26.5	7.4	27.92 %
4	33.5	9.3	27.76 %
	27.2	7.6	27.94 %
	29.8	7.2	24.16 %
5	42	12.3	29.29 %
	38.6	12.2	31.61 %

It is seen from the table that all except one test is in the range of 20-30% water content, with one of the tests on the quick clay being slightly over. This is well withing the standard range of water content for Norwegian clays which is the range 20-50%. It is interesting that the coarser soil should have lower water content than the rest, but sample 1 does not have significantly lower water content than the rest of the samples. The only clear result is that the lower portion of sample 5, which as mentioned is quick clay, has the highest water content. This is to be expected given that the sample was visibly wetter than all other samples in addition to the fact that quick clay normally have a high water content. (NTNU 2017)

6.3.2 Fall cone

Following below are the results from fall cone testing of the five samples from P_1P_2 borehole. The headers vary between vertical and horizontal in order to maximize the readability of the results.

Table 3: Fall cone test

The test is executed with sample both undisturbed (u) and remoulded (r)

Sample nr	**Depth [m]**	**Cone mass u [g]**	**Cone penetration u [mm]**	**Cone mass r [g]**	**Cone penetration r [mm]**	**Su [kPa]**	**Sr [kPa]**	**St**
1-1	3.23-3.28	400	1.83	400	8.0	933.98	49.05	19.04
1-2	3.48-3.53	400	2.00	400	6.8	784.80	68.90	11.39
2-1	9.04-9.09	400	7.83	100	8.7	51.16	10.45	4.90
2-2	9.29-9.34	400	3.67	100	6.0	233.49	21.56	10.83
2-3	9.47-9.52	400	4.50	100	6.3	155.02	19.57	7.92
3-1	13-04-13.09	400	6.00	400	9.0	87.20	38.76	2.25
3-2	13.29-13.34	400	3.33	400	8.5	282.53	43.45	6.50
3-3	13.5-13.55	400	3.50	400	8.7	256.26	41.79	6.13
4-1	22.04-22.09	400	4.83	400	13.7	134.38	16.81	8.00
4-2	22.29-22.34	400	4.17	400	16.0	180.82	12.26	14.75
4-3	22.41-22.46	400	3.50	400	13.0	256.26	18.58	13.80
5-1	40.09-40.14	400	9.00	10	16.0	38.76	0.10	374.58
5-2	40.25-40.30	400	10.00	10	20.0	31.39	0.07	474.07
5-3	40.45-40.50	400	6.50	10	15.0	74.30	0.12	631.16

As the table above shows, samples 1 through 4 all have high strength, both undisturbed and remoulded. For the fall cone test to to give "good" results for shear strength, it is required for the cone peetration to be between 4 and 20 mm. This is because the formula for shear strength is dependant on this penetration. It can be seen that for the tests that gave a smaller penetration than 4mm, have an unrealisticly high shear strength, and the smallest difference in penetration gives a hughe difference in shear strength. This can be seen for sample no. 1-1 and 1-2, where the penetration difference is 0.17 mm, but the shear strength difference is around 150 kPa.

Nevertheless it is clear that the samples 1-4 have a high shear strength, both undisturbed and remoulded. While the fifth sample is quick clay. The remoulded shear strength is well below 0.5 kPa, which is the threshold for quick clay. It is also worth noting that the quick clay sample actually has a relatively high undisturbed shear strength, which leads to a very high sensitivity.

6.3.3 Uniaxial test

Followig is the results from uniaxial testing of the samples. One test was carried out for each of the samples.

Table 4: Uniaxial test

Sample no	**A_0 [mm^2]**	**Axial deformation [mm] = [%]**	**Pf [kg]**	**Max load [N]**	**σ_1f [kPa]**	**Su [kPa]**
1	2290.22	6.00 %	55	539.55	221.45	110.73
2	2290.22	10.00 %	28	274.68	107.94	53.97
3	2290.22	8.00 %	45	441.45	177.33	88.67
4	2290.22	5.00 %	43	421.83	174.98	87.49
5	2290.22	8.00 %	30	294.3	118.22	59.11

As is seen in the table, the shear strength is by far highest in sample 1. This is to be expected given that this sample visibly contained elements found in top soil. Surprisingly sample 5 does not have the lowest shear strength, but sample 2 does. When looking at the results from the fall cone test it is clear that the strength near the top of sample 2, where the uniaxial test also was completed, was significantly softer than the lower part. It is also not definite that the undrained shear strength is in fact lower for sample 2, since the test results rely on visual evaluation of the graph generated, but they are in the same area.

6.3.4 Grain size distribution

Grain size distribution was completed with wet sieving method. The results from wet sieving was very similar for all samples which was that a very large portion of the sample passed through all sieves with very minuscule amounts retained on each sieve. For the samples 2, 3 and 4 the amount of retained material $> 0.63mm$ was between $10 - 20\%$ while for sample 5 the amount retained was around 1%. Still it´s a large part of every sample that went through all sieves, and the classification for all samples are clay, or silty clay for samples 2,3 and 4 because of the amount retained.

The wet sieving was not completed for sample no 1 at 3m depth. This sample had the largest visible part of soil types not being clay as well as rocks in the sample. Sample 1 is classified as topsoil, consisting of sand, silt and clay.

6.3.5 Density

Table 5: Density and Unit Weight

Density	Sample 1	Sample 2	Sample 3	Sample 4	Sample 5
Ring [g/cm^3]	1.98	2.02	1.96	2.00	1.92
Cylinder	2.03	2.02	2.28	2.04	2.06
Average	2.01	2.02	2.12	2.02	1.99
Unit weight, γ [kN/m^3]	19.67	19.82	20.80	19.82	19.52

The density calculated using the density ring as well as the sample cylinder itself is presented above. The average density is calculated to get the best representative density. The unit weight is calculated using the average density and gravitational acceleration.

The unit weight is very similar for all samples/depths ranging from 19.5 to almost 21. This is very much in the expected range for our samples consisting of silt, sand and clay. The unit weight is here also calculated to use it in the CPTU-sheet from statens vegvesen to get a more detailed layering indication, shown in figure 26.

6.3.6 Liquid limit

Underneath a table with the different samples liquid limit is presented. Only the sample number and the liquid limit is presented.

Table 6: Liquid limit

Sample no	w_L
1	36.50 %
2	34.00 %
3	39.50 %
4	33.50 %
5	25.60 %

The liquid limit is mostly in line with what to expect from the soil tested. Typical Norwegian marine clays have a liquid limit of around 40±5%. When the test was executed, there were some difficulties with getting the sample to the correct water contents in order to get the desired number of drops. Therefore for some of the samples, some of the number of drops are slightly outside of the range desired, and can effect the resulting liquid limit obtained. Still the results are close to what is to be expected here. One can also see that the liquid limit for sample 5 is lower than its water content, which is characteristic for quick clays. (NTNU 2017)

6.3.7 Plastic limit

In the table below, the results for plastic limits are presented.

Table 7: Plastic limit

Sample no	w_P [%]
Sample 1	22.92
	26.92
Sample 2	20.93
	19.23
Sample 3	24.56
	28.81
Sample 4	21.09
	23.66
Sample 5	22.41
	21.62

The values fall within what is normally expected for typical Norwegian clay. For marine clays the expected values are $22 \pm 5\%$ which covers all results except one from sample 3. Due to the nature of the test being based on an approximation and eyesight alone, some deviation is to be expected without it meaning the soil itself is deviating from what is normal. (NTNU 2017)

6.4 Plasticity and liquidity index

With both the plastic and liquid limit, the plasticity and liquidity was calculated. The results are presented in the two tables below.

Table 8: Plasticity

Plasticity [%]	
Sample 1	13.58
	9.58
Sample 2	13.07
	14.77
Sample 3	14.94
	10.69
Sample 4	12.41
	9.84
Sample 5	3.19
	3.98

Table 9: Liquidity index

Liquidity index	
Sample 1	0.30
	0.01
Sample 2	0.54
	0.59
Sample 3	0.16
	0.03
Sample 4	0.56
	0.44
Sample 5	2.07
	1.85

Norwegian clays generally are considered to be of low plasticity and the results are very much in line with this. The low plasticity is classified as below 10, and medium plasticity is the range of 10-20. All results show either below 10 or are at the lower end of the medium plasticity range. The plasticity for samples 1-4 are very similar, with the quick clay sample 5 having extra low plasticity. (NTNU 2017)

Though the liquidity results for the different samples in some cases deviates a bit from each other, they are still in the expected range for the soil type found. Samples 1-4 all lie in the range of 0-1, while the quick clay in sample 5 have a liquidity index > 1. The liquidity index over 1 is a result of the samples water content being higher than the liquid limit, which is special for quick clay. Considering even the limitations of the tests, all results in the tables above is within what is to be expected.

6.4.1 Resistivity pore water method

The resistivity results from the pore water method seen below was decided to be discarded. This because they were deemed incorrect. They deviated significantly from all other resistivity results obtained and also did not coincide with what values to be expected for the soil. It unfortunately not possible to verify this by testing a substance with known resistivity to check the deviation the device produced and ultimately the decision was to neglect the obtained results in favor for the other seemingly correct results.

Table 10: Resistivity and salt content, pore water method

Sample nr	**Depth**	**Salt content [g/L]**	**Resistivity [Ωm]**
2	9.4	0.653	10.4
4	22.4	0.374	18.2
5	40.4	0.463	14.7

As seen in the table, the resistivity doesnt change much, staying inside the range of 10-20. Even if they in fact are within the range presented in table 1, they are significanly lower than the other results, and does not vary as much as expected given the different soil properties at the different depths. It also is noteworthy that it didn't just deviate from some of the other results, the other results showed very much the same, so this test was the only outlier. Given that it is assumed the resistivity values gotten from the device is inaccurate, the salt content gotten from the same machine is hard to trust.

6.4.2 Resistivity current method

Table 11: Electrical Measurements

Sample nr	**U** [V]	**I** [mA]	**A** [m^2]	**L** [m]	ρ [Ωm]
2	6.62	5.15	2.2902	0.05	59
3	8.89	5.33	2.2902	0.05	76.4
4	9.8	4.82	2.2902	0.05	93.13
4	9.7	5.14	2.2902	0.05	86.4
5	9.93	9.05	2.2902	0.05	50.26
5	9.62	9.25	2.2902	0.05	47.6

Above is the results from labtesting the different samples resistance to electrical current. These are resistivity results from samples only from P_1P_2. The results were obtained from using the method described in figure 2.

7 Discussion and comparison

7.1 Resistivity measurements and ERT

The different resistivity measurements have given different results. The biggest difference is found when looking at the resistivity from the test utilizing pore water. From the pore water examination the resistivity was significantly lower than all the other tests. On the other hand, the lab test measuring the resistance of the soil which further was calculated to resistivity, correlated well with the RCPTU done in the field. It is therefore assumed that the pore water test have provided inaccurate results. This can be because of several reasons, but probably is because of damaged or not calibrated equipment. When plotting the RCPTU next to the lab results from different depths, the alignment is almost identical. This is seen in figure 27a.

Plotting resistivity results from ERT over the RCPTU as done with the lab results above is also done. When doing this it is essential to assess what coordinates to look at when gathering the resistivity results from ERT. Since the total sounding and RCPTU is not in fact directly at the same spot as the ERT-line, a decision was made. The drilling results were for P_1P_2 moved to the intersection between ERT profile 1 and ERT profile 2. This is only the case for P_1P_2, since the $P5_1$ RCPTU is approxomately directly at the ERT 5 line. It was moved to this intersection in order to use resistivity values from both ERTs at the exact same coordinates for comparison with the other results. The distance from the drilling cite and the ERT intersection is 26m, seen later in figure 28. In order to get enough results from the ERT file, the resistivity values were gathered from coordinates within 1m of the intersection. The values obtained from ERT 1 and ERT 2 is plotted with the RCPTU resistivity as well as the results obtained in the lab in figure 27b.

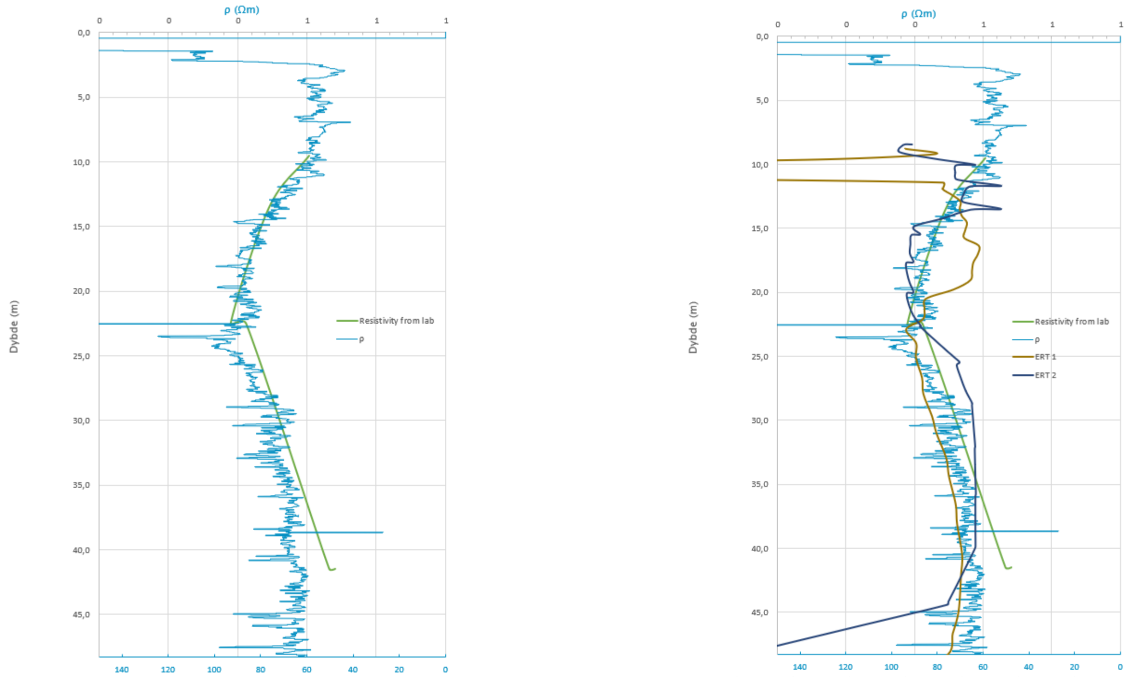

(a) Resistivity RCPTU and lab

(b) All results

Figure 27: Resistivity from RCPTU, ERT and lab

As shown in the plot, the resistivity values seem to correlate better with depth. Below 20m all resistivity values are relatively alligned with each other. Above this the results are a bit more scattered, a reason for this may be because the layering is more homogeneous further down than near the top. It can also be because of the different soil types further up. It was seen in the lab that the silt and sand content was higher at the samples above 20m depth while the deep samples was near 100% clay. There is also the fact that the RCPTU and the samples are not at the exact same coordinates as the ERTs to consider as a factor of inaccuracy.

With all the above results together, the general resistivity division can be made and seen in comparison with what soil is to be expected at these values. In addition to what soil in fact is present, proven in the lab.

Because of only having sample from one borehole, and not three as planned, the geotechnical lab results for comparison with the geophysical results are somewhat lacking. For P_3 and P_7, only total sounding is available to compare with ERT visual plot. At P_5 both total sounding and RCPTU are compared.

7.2 Correlation geophysical and geotechnical results

7.2.1 P1P2

For P_1P_2 the borehole is located 25m away from the intersecting ERT-profiles. In order to interpret together with the ERT results, the drilling is drawn to the intersecting ERT profiles as shown in the figure below. The distance is around 26m.

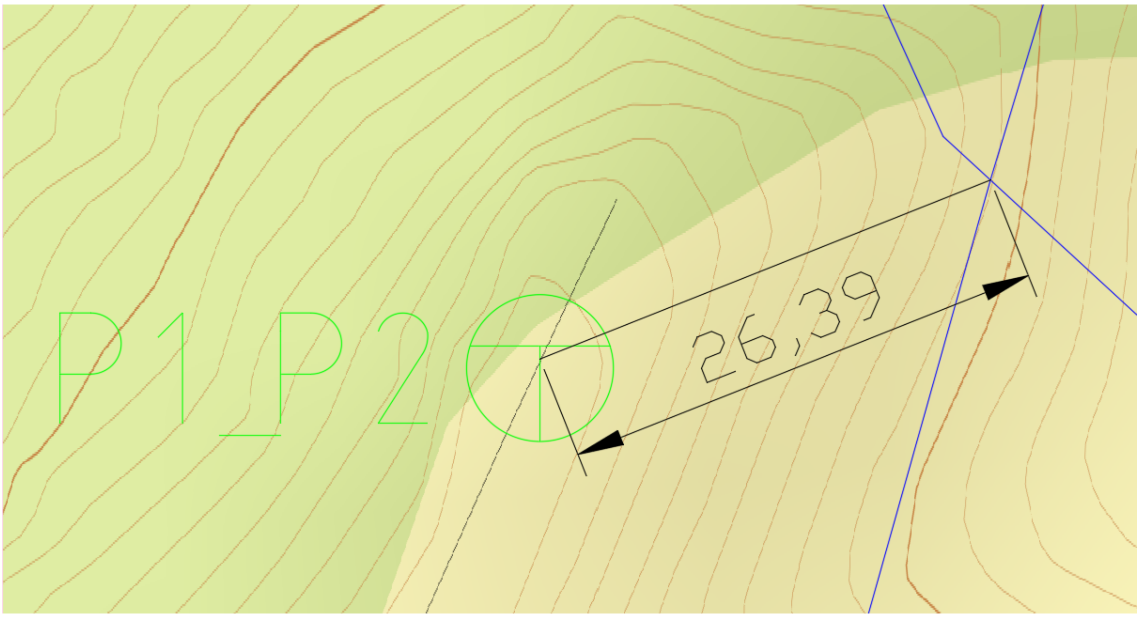

Figure 28: Distance p1p2 drilling and p1p2 ERT

The plots of the total sounding with the resistivity results from ERT 1 and 2, are shown in figures 29 and 30.

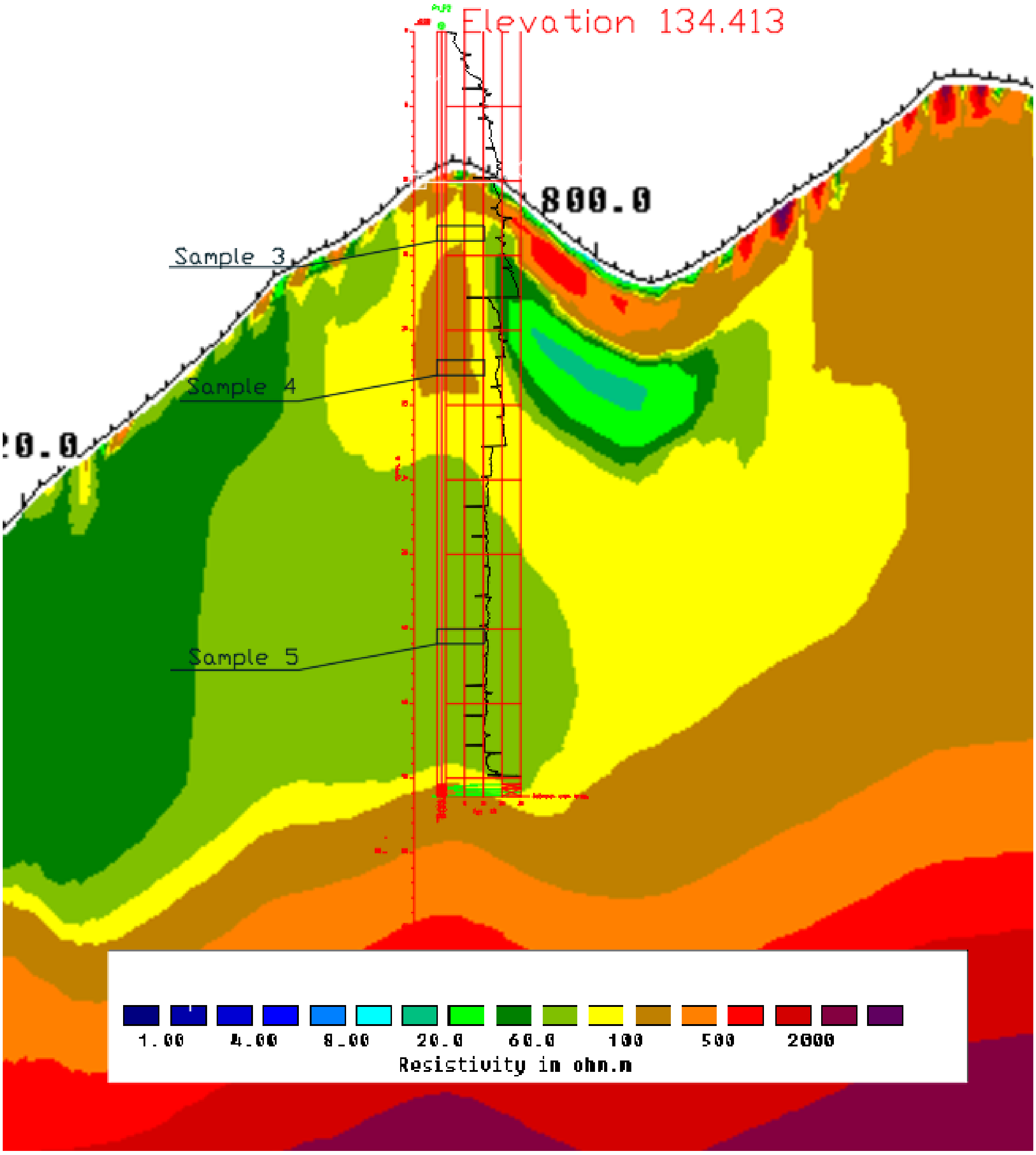

Figure 29: Total sounding P_1P_2 and ERT 1

The total sounding is not starting at the ground level of the ERT because of a difference in elevation. Assuming that the layers are somewhat horizontal, it would be best to compare the sounding and ERT at equal elevation, which is obtained by rising the total sounding above the ERT. The elevation difference at the intersection (the intersection between the ERT profiles are at the location of the total soundings in the figures above) is 8,5m.

From the top the ERT indicates coarse material with high resistivity, backed up by both the drillings and the lab results. The drilling shows high resistance and from the lab it is made clear that the material is top crust. This crust containing silt, clay and sand with high strength. Near the top the ERT shows several different resistivity levels at close proximity to each other which indicates not homogeneous soil. This is typical for top crust, and was also seen from the lab results. There were small pieces of rock found in sample no 1 and 2, as mentioned earlier. Near the top the samples also had a larger content of sand which generally have a higher resistivity than silt and clay. This mixture of soil types and a high strength is also seen in the total sounding plotted with the ERT. The drilling resistance is visibly higher near the top of the ERT.

The drilling resistance drops at around 28m depth (measured from top of total sounding, around 20m depth from top ERT), right before the resistivity also drops. This is right before the transition from yellow (80-100Ωm) to light green (60-80Ωm) looking at the ERT. The lab results show that sample 4, from 22 m depth, was softer than the previous samples but not to the point of being quick. It still had significantly higher remoulded shear strength than quick clay. This sample is, using figure 29, in the middle of the yellow area with resistivity between 80 and 100, just a few meters before the drilling resistance drops drastically. The drop in resistance at 28m is continuous until around 50m deep (at the bottom of the light green area, when it again transitions into yellow and then brown, 100-300Ωm). This layer, from 28-50m is assumed to be homogeneous, this assumption drawn from the fact that the RCPTU, ERT data and total sounding indicates it. This continuous layer is labelled quick clay. The lab results prove that at 40 m depth there is quick clay, this together with the other results gives the basis for this conclusion.

As with ERT 1, a comparison is done with ERT 2. Since the ERT profiles will have the same elevation in the intersection point, the total sounding is also here elevated above the ERT profile as seen below.

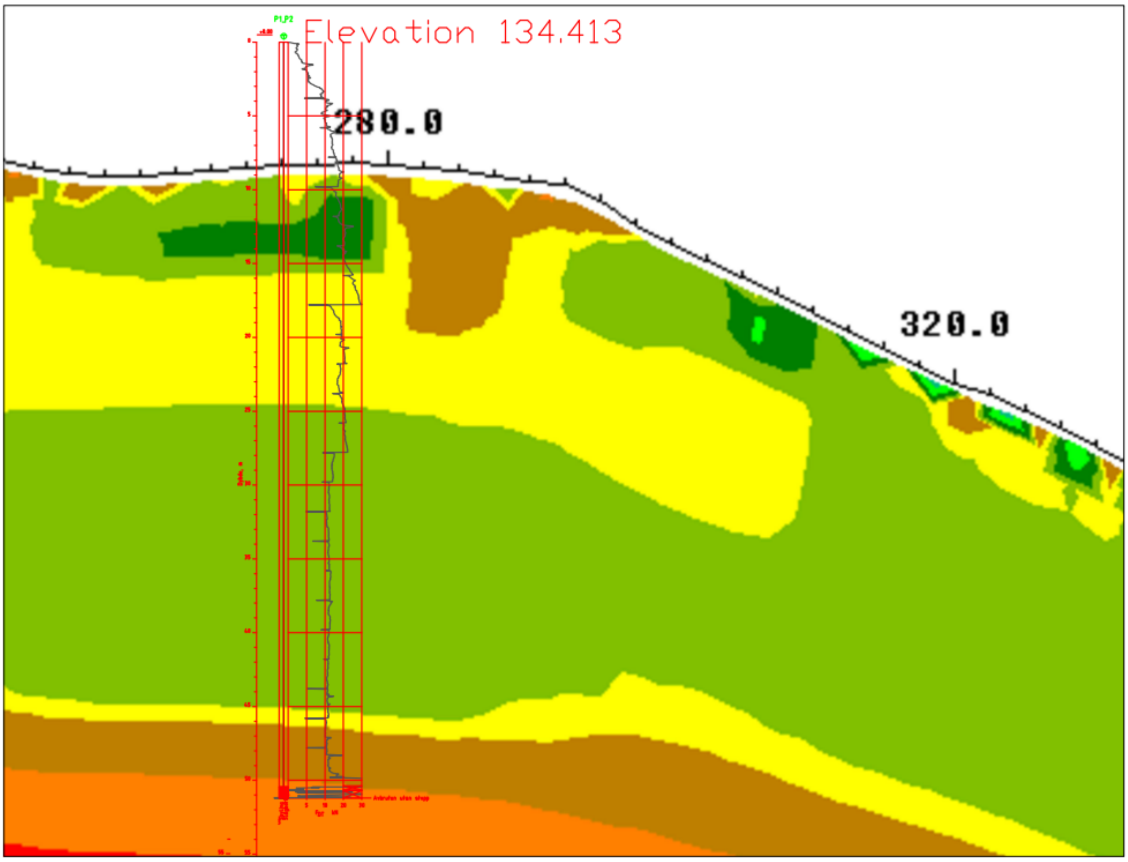

Figure 30: Total sounding P_1P_2 and ERT 2

The ERT here is a bit more "clean" than ERT 1, with less small layers and more homogeneous horizontally. Much of the same results can be interpreted from this figure above as in figure 29. Near the top, as well as the dark green area (40-80Ωm), into the start of the yellow area (80-100 Ωm) has a relatively high resistance. No hammering or flushing was used, but it is clear that the resistance increases with the depth which is typical for none sensitive soil. A few meters into the light green area (60-80Ωm), we again find the depth where the resistance drops. The drilling resistance stays low throughout the entire light green area, through the small yellow layer (80-100Ωm) and then increases around the middle of the brown layer (100-300Ωm). Given that the total sounding is not directly above the ERT line it is fair to assume some discrepancy in the depth to the different layers, but the ERT layers still seem to coincide well with the different resistance shown at different depths. This has been the case for both ERT 1 and 2, so there definitely seem to be a connection between the layers presented by ERT data and the difference in drilling resistance from the total sounding.

7.2.2 P3

Below is the total sounding $P3_1$ plotted near the start of ERT line 3.

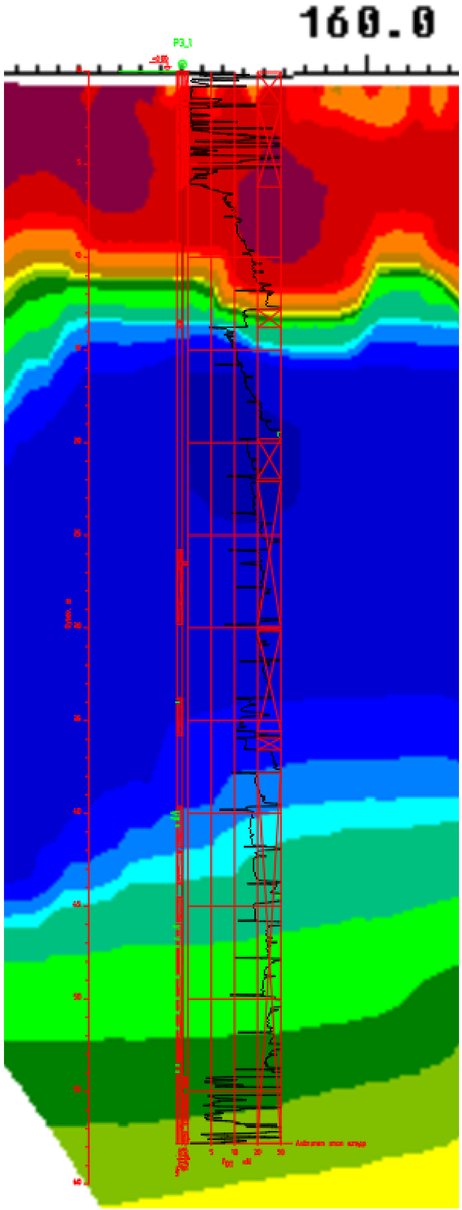

Figure 31: Total sounding $p3_1$ and ERT 3

In $p3_1$ shown above it is clear that the drilling resistance is very high for most depths. For the top 10 meters, where the ERT is red and purple it is espessially high. Red and purple represents resistivity values over 500 Ωm which is common for stiff topsoil containing rocks and hard material. From the total sounding the coarse top soil needing flushing and hammering stops at 6m, but there might very well be a gradual transition into the next layer. This means that even if the ERT plots a deeper topsoil, the mechanical properties of the soil itself may make the ERT test not pick up the transition of layers at 6m, and interprets it to go as low as 10. This is probably because of the distance between the electrodes as explained earlier which may lead to inaccuracy in the resolution. It was used both water flushing and hammering up until 6m depth in order to penetrate. At 6m, when the flushing and hammering stopped the total sounding shows how the resistance steadily grows until the end of the red area ($> 500\Omega$m) where it is almost at 30kN.

The drilling resistance drops for a bit when the ERT shows an abrupt transition into several thin layers with lower resistivity underneath the red top soil area (20-500Ωm). These thin layers in the ERT plot are only about 2 meters of depth. There was also is used some flushing at the end of the thin layers, so it still seems to be stiff soil. For the rest of the depth, from the start of the blue area(0-10Ωm), until the end of the total sounding, the resistance is high. It is sporadically used flushing when the resistance reaches 30kN. Even where the resistivity is different shades of green(10-80Ωm), which is one of the assumed areas where we could find sensitive clay, the resistance is so high that it requires almost continuous flushing in order to penetrate. Nearing the end it also required some hammering which definitely shows the soil is stiff.

Total sounding number $P3_2$ below is showing much the same pattern as $P3_1$. The layering from the ERT, meaning the different color layering, is similar but not exactly the same for them both. Here in $P3_2$ the usage of flushing is even more frequent, with using it at almost the entire depth. The soil seems to be more homogeneous from 25m depth and down, with the total sounding giving a relatively consistent resistance with flushing from 25-40m depth.

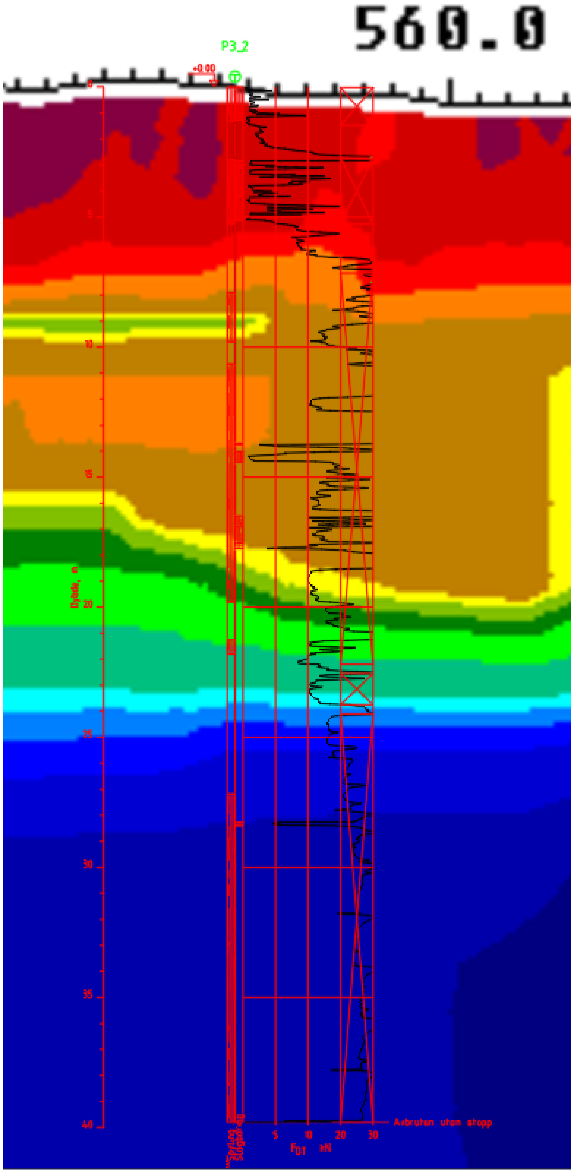

Figure 32: Total sounding $P3_2$ and ERT 3

Up til 18m depth it shows a high resistance even when flushing. There are some drops in he resistance but they coincide with when hammering was used so the soil here is very stiff. Still the area where neither flushing nor hammering was used, is where the ERT have the different shades of green as well as the start of the blue area(5-80Ωm). The resistance is still in this area considerable but flushing and hammering was not necessary. We therefore expect a bit softer soil here.

7.2.3 P5

$P5_1$ is the only sounding going through almost only one layer looking at the ERT plot, seen below.

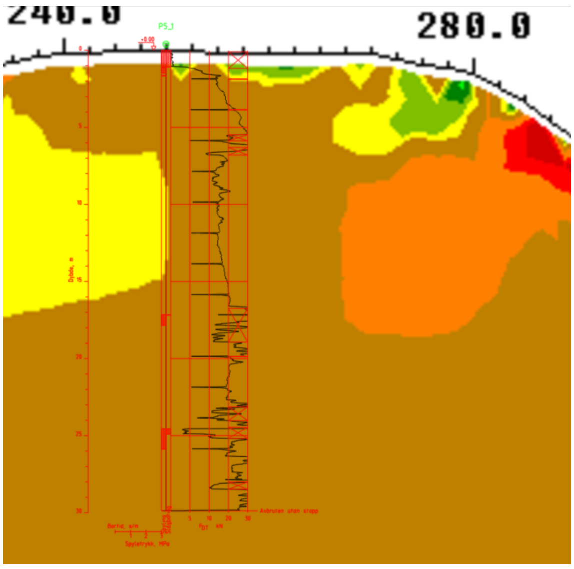

Figure 33: Total sounding $P5_1$ and ERT 5

Even if the ERT is mostly homogeneous light brown (100-300Ωm) throughout the depth of the sounding, the sounding itself shows some layering. The top soil is not as deep as some in some of the other areas, but there was used both hammering and flushing at the start of the drilling.

After the top soil, there seems to be some mix of silt, sand and clay, with high resistance until about 12m depth. The resistance then drops and has a slow increase in resistance until 16m depth. Then the resistance is very high, also needing some flushing and brief hammering, until 20m depth. From 20-22m depth there seems to be a softer layer seen clearly in the total sounding. This is not in the range of leached clay assumed earlier, but just outside, since light brown indicates resistivity from 100-300Ωm. After this layer the resistance increases again and stays high until the end. There was also a need for flushing and hammering in this last part. So even if the ERT is homogeneous light brown, there still seems to be layers here, also a possible small more sensitive area at 20m depth.

7.2.4 P7

The total soundings $P7_1$ and $P7_2$ are also plotted with the ERT profile 7 data, shown under.

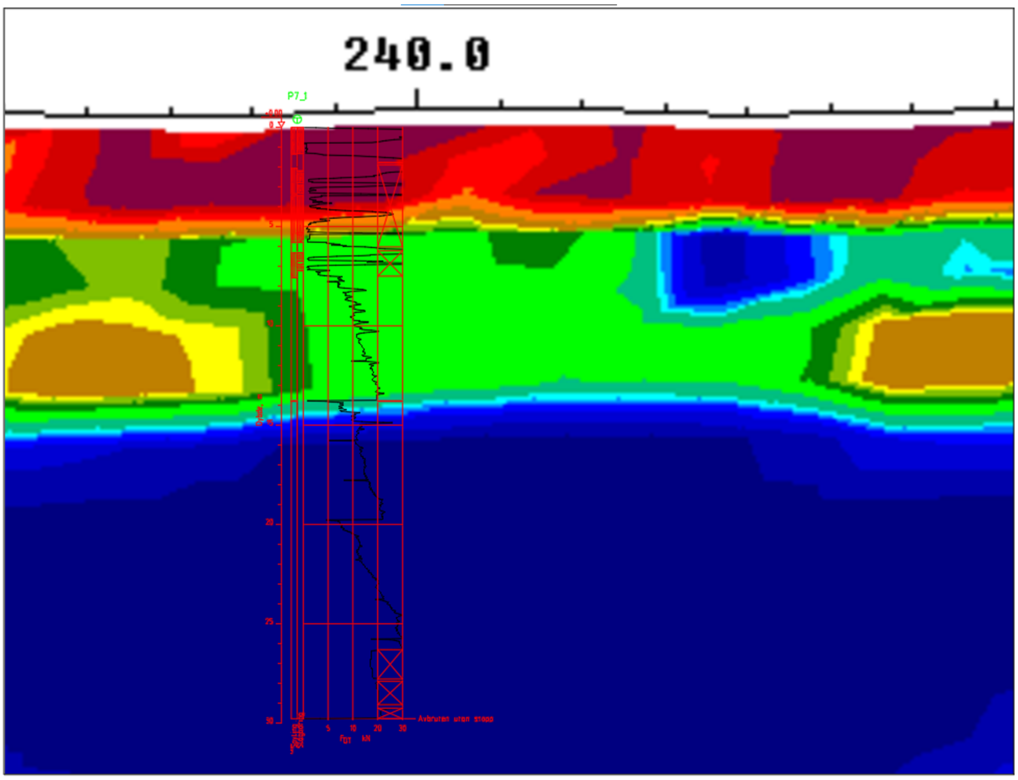

Figure 34: Total sounding $p7_1$ and ERT

The ERT here can be seen to have three major layers. The first one down to around 5.5 m depth. The total sounding shows a layer of coarse material down to 7.5m. So they both pick up the coarse layer, but the total sounding shows it goes a few meters deeper than the ERT. Both flushing and hammering were used most of the depth down to 7.5m so the soil is definitely coarse. Further through the light green area of the ERT the soil seems homogeneous. This is also seen from the total sounding, which shows a steady increase in resistance up until 14m. There was not used any flushing or hammering and is interpreted as a layer of solid clay. At the end of this layer some flushing was used without pushing the drill rods down in order to wash the drill rods and eliminating some friction along the rods. From inspecting the drill rods the clay layer also seemed to have a small presence of silt and sand.

Further into and through the blue layer(1-6Ωm) the soil also seems homogeneous from both ERT and total sounding. The soil here is interpreted as firm tough clay. The clay was tougher through the blue area than the light green. This was also noticed in the field. There was a need to use flushing at some of the rod changes because of the large friction that was built up along the rods when penetrating.

$P7_2$ a bit further down along the ERT line is also plotted in figure 35.

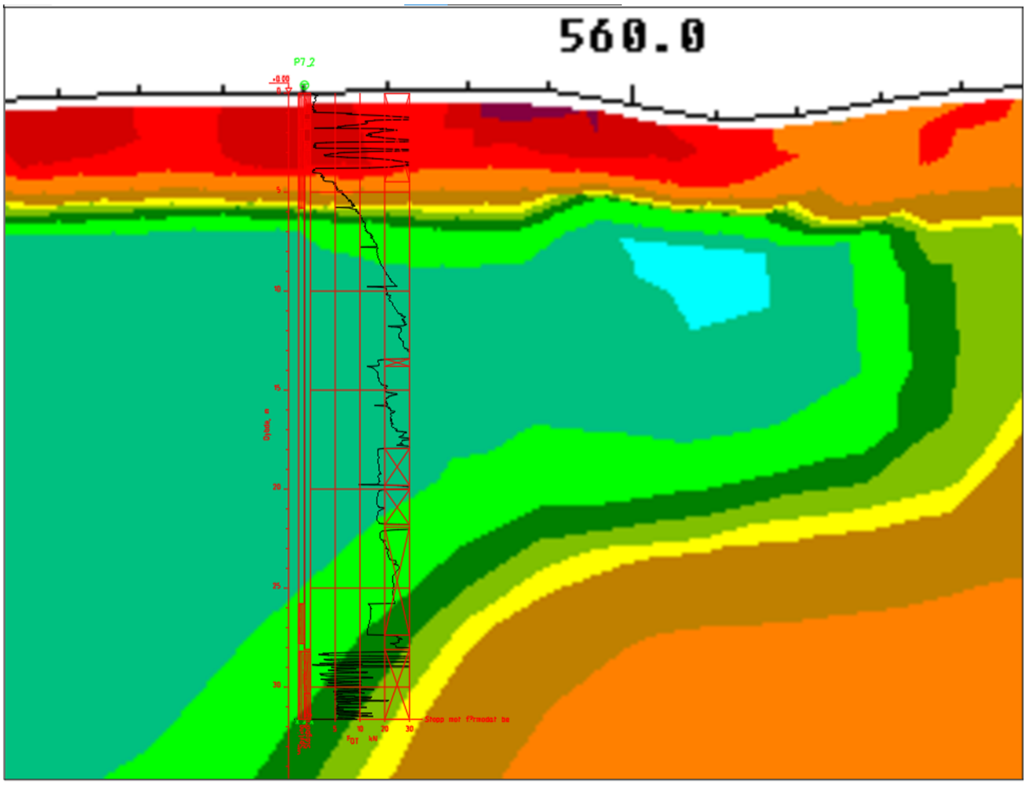

Figure 35: Total sounding p7_2 and ERT

The coarse top soil is also here clear from both ERT and total sounding down to 4.5m. The ERT here, as for $P7_1$, shows the coarse layer going a few meters deeper than the total sounding.

Underneath the top soil, the soil seems to be firm and homogeneous until around 15m depth. The resistance is slowly increasing with depth up until this point. Some drops in resistance is seen, but coincide with flushing when changing rods. Further the soil seems to have some small layers causing the resistance to fluctuate, bot looks mostly homogeneous and firm here as well until 28m depth, needing some flushing near the end to not exceed 30kN resistance. The sounding then shows a layer of coarse material, before hitting bedrock at 29m depth. This is interesting because the ERT doesn't indicate bedrock at this depth, even if the ERT is transitioning into coarser layers a bit deeper. It is clear from the ERT that there seem to be an "underground hill", meaning that the bedrock is at a significantly lower depth to the right of the sounding than at the left. The curved layering in the figure above is showing this. This can lead to that an inaccurate placement of the sounding can have a large impact of the depth to bedrock. Given that the sounding is placed with detailed coordinates, this seems unlikely. Then the possible answer is that the ERT might have some inaccuracy in the placement of the deep layers, which seems plausible given that the accuracy lessens with depth. This in addition to the mentioned possible inaccuracy because of the electrode distance in the test itself.

7.3 Layering

The results are used to make layering profiles for the places that minimum have both drillings and ERT in place. The layering at P_1P_2 will be the most accurate because of the amount of results available to interpret.

7.3.1 P1P2 layering

The results from labwork shows the parameters for the different depths, and in conjunction with RCPTU, total sounding and ERT gives the opportunity to interpolate between the results to give a detailed layering profile seen below.

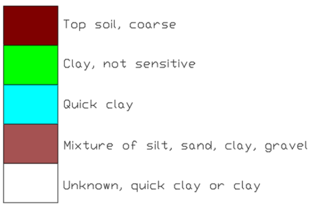

(a) Color legend

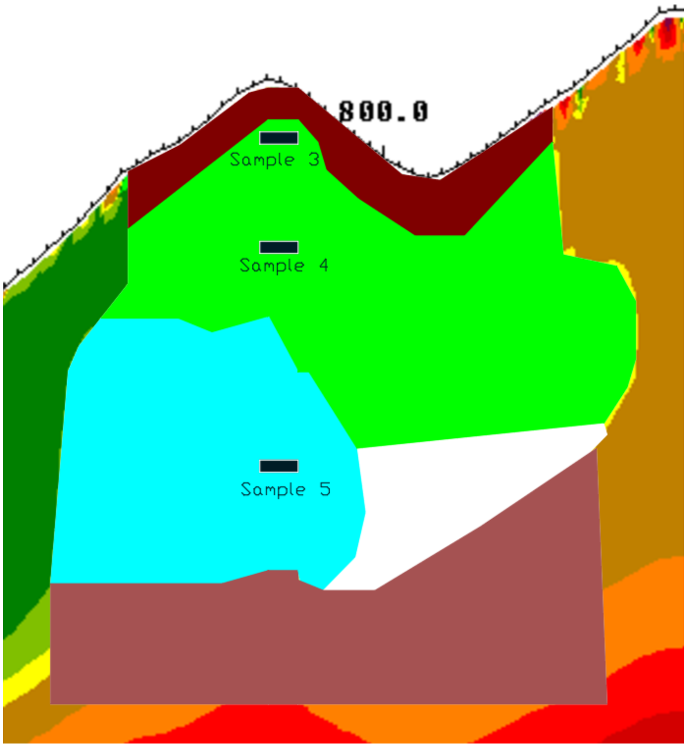

(b) Layers

Figure 36: Layering P_1P_2

The layering based on all results show a lot of what was expected. Since there are only drillings and samples at one location for ERT 1 and 2, the width of the layering is difficult to establish with pinpoint accuracy. The layering at the spot shown in figure 29 will have the most accuracy, and the expansion of the layering horizontal is based on ERT alone. Given that the layering coincide well with the layers shown in the ERT, the accuracy should be good. It is seen in the layering that the quick clay is found where the ERT has a light green area (60-80Ωm). The quick clay layer seem to start exactly where the ERT shows a transition between yellow and light green zone. Even if both yellow and light green can represent leached clay, the lower resistivity values for light green represents a lower presence of silt. For this area, it can be said that the light green area from ERT (made light blue in the layering profile), which can mean sensitive clay, in fact were quick clay. It is important to mention that there were also green areas where there wasn't quick clay. So it can be said that in this particular situation the ERT did have some light green areas that didn't correspond to sensitive soil, but there was not found any sensitive soil that wasn't in a light green area.

7.3.2 P5 layering

The layering in $P5_1$ is based on total sounding, RCPTU as well as ERT 5. The layering results from these different tests are presented in Appendix A.

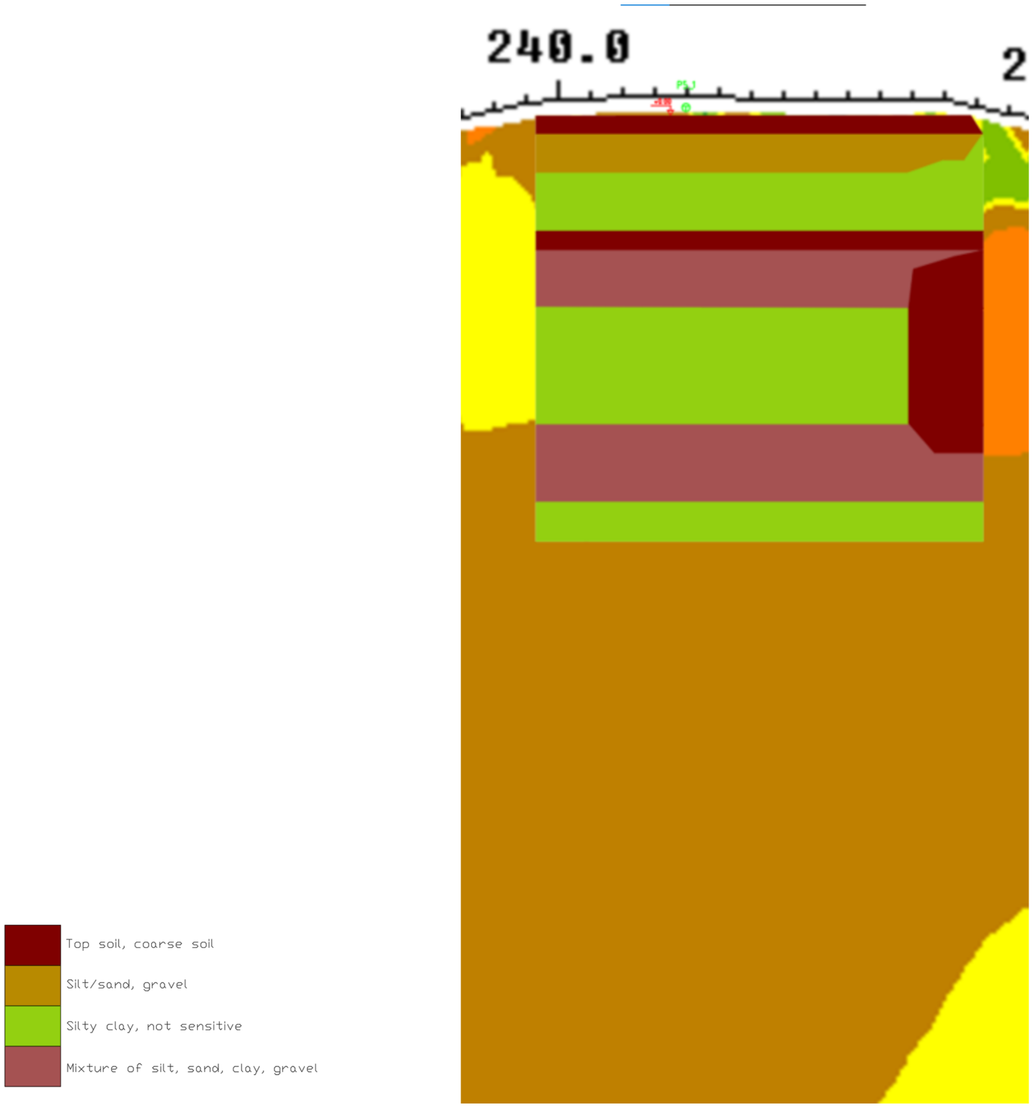

(a) Color legend

(b) Layers

Figure 37: Layering P5

7.3.3 P3 layering

The layering in $P3_1$ and $P3_2$ are based on the total soundings as well as the ERT data.

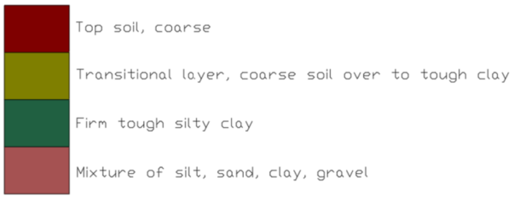

(a) Color legend

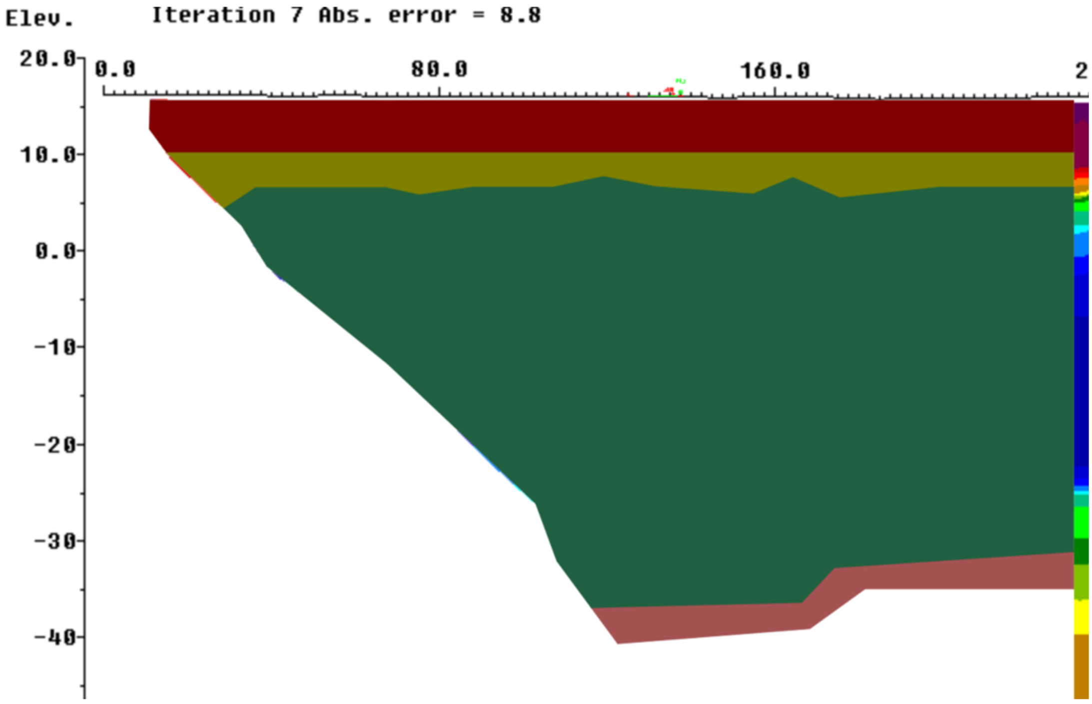

(b) Layers

Figure 38: Layering $P3_1$

The black dots in the profile for $P3_2$ below shows where the total sounding indicated gravel. It was heard during fieldwork how the drill hit gravel at this depth. The dots are concentrated where the drilling is placed and an extension is illustrated how the gravel might stretch horizontally.

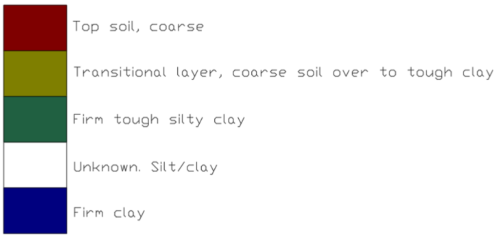

(a) Color legend

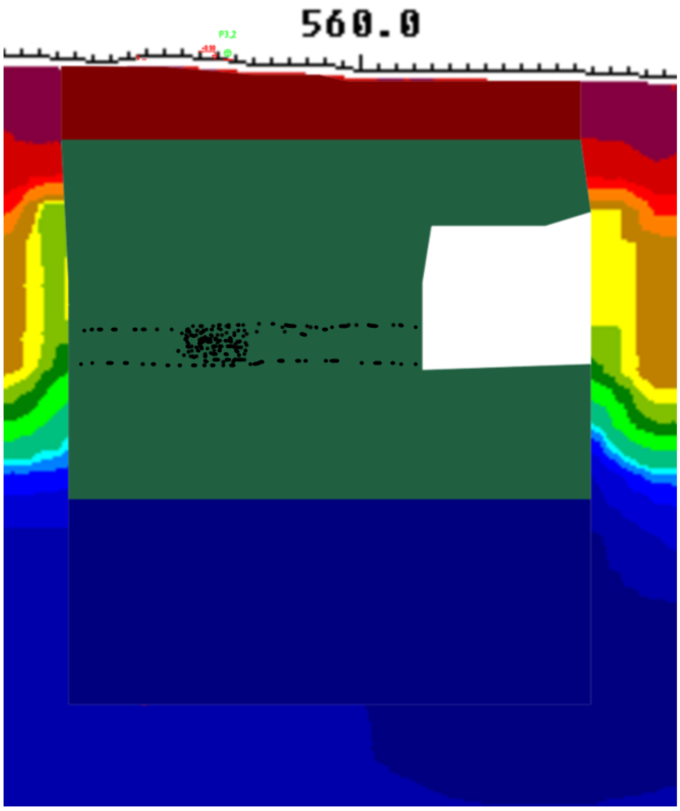

(b) Layers

Figure 39: Layering $P3_2$

7.3.4 P7 layering

The layering in $P7_1$ and $P7_2$ are also based on only total sounding as well as ERT.

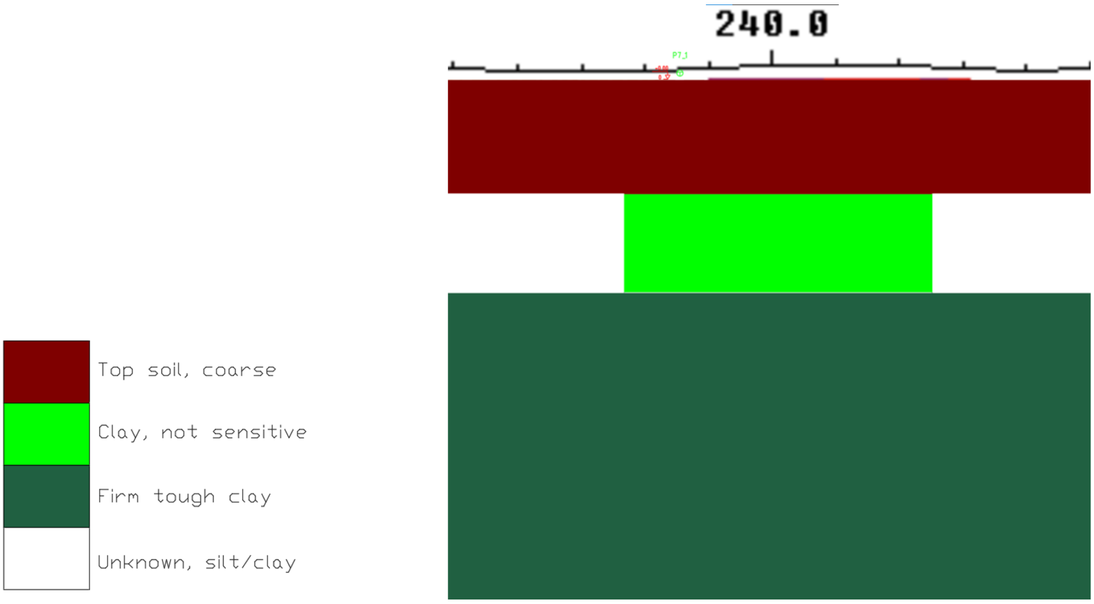

(a) Color legend *(b) Layers*

Figure 40: Layering $P7_1$

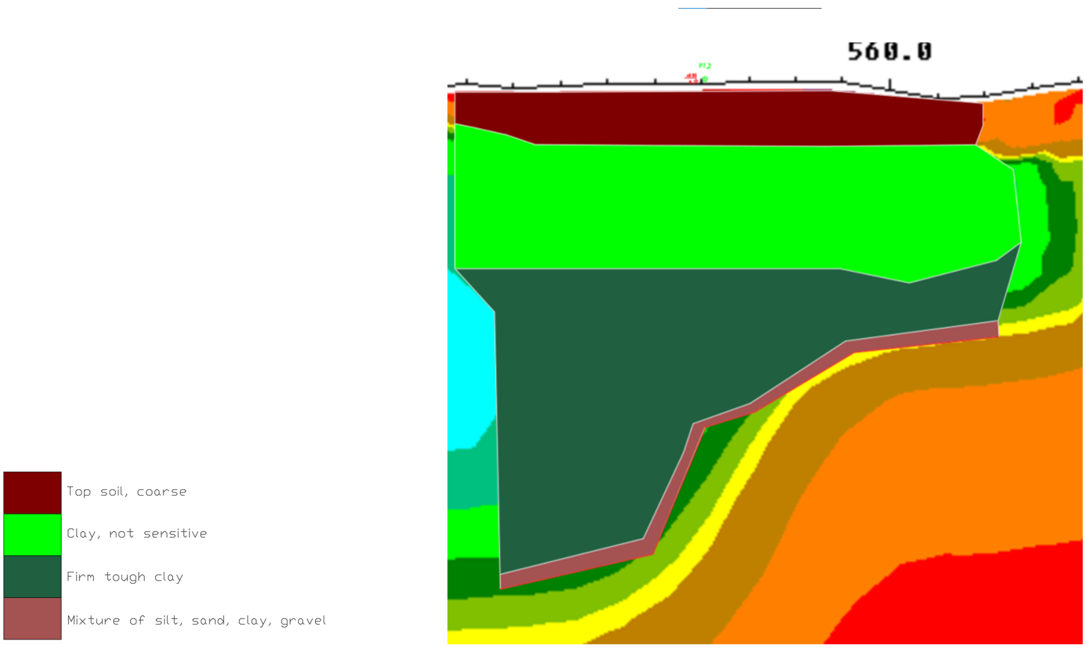

(a) Color legend *(b) Layers*

Figure 41: Layering $P7_2$

7.4 Limitations

The are different limitations with the layering profiles. The layering extends horizontally with a different width in each profile. This because the horizontal extension is mostly based on how homogeneous the layers seems to be in the ERT in combination with the total sounding. This may lead to some discrepancy with the actual soil present located next to the tests. The profiles that have two soundings along the ERT lines were too far apart to interpolate the layering between them without the risk of being to inaccurate.

It is difficult to accurately determine in detail what soil is present at the different depths without samples, so the different layers may deviate some from the actual soil, but is an estimation based on the available results.

Some small layers with slightly different values from the layers presented were also not included in the profiles. This was exclusively for small layers of coarse soil, so no sensitive areas were excluded.

8 Conclusions

Since the amount of samples is insufficient it is difficult to conclude wether the geophysical methods enable the reduction of boreholes in general. However it is shown for this particular case that the ERT gives a good suggestion about the type of soil present. It is clear that the high resistivity areas correlate well with stiff soil seen in total soundings, and vice versa. One of the samples shows this well where the ERT indicated leached clay, possibly quick, where it was proven quick clay. The ERT had several areas with light green color, indicating the possibility of sensitive clay, where sensitive soil was not present. But at the location the quick clay was found, the ERT had marked it as a possibility. Not all indicated areas were sensitive, but all proven sensitive areas were indicated. There is the case of a thin layer in drilling $P5_1$ where the resistance during the total sounding dropped for a bit, which could mean this is a sensitive area, without being definitive. This area was just outside the estimated range of leached clay. Even so, it seems the ERT profile gives a good indication on where one can expect to find sensitive soil. In all areas where other results were available these backed up the interpretation from using ERT, except for the one mentioned where the ERT showed non sensitive soil.

For this project the soundings were based on the ERT profiles, and the sampling and RCPTU was based on them both. This was in retrospect a good solution, where the ERT data did in fact show the potentially hazardous areas, backed up by the results from field and lab.

Based on this project, it can be concluded that the method of first completing geophysical tests and then geotechnical tests based on the results obtained can be a good approach to delineate the possible hazardous areas as well as reduce the amount of drillings needed. The level of detail from ERT seemed to coincide well with what the other results showed and is therefore considered good. It is important to note that this method of mapping is somewhat limited to rural areas in order to maximize the efficiency and advantage of the large mapping capability of ERT, as well as ensuring that the completion of ERT is possible with minimal disturbances. (Lundström, Larsson, and Dahlin 2009) This is the case for the project area in Orkdal, with large open fields.

9 Recommendations for further work

Given that the scope of the project was somewhat narrowed down because of the difficulties in the field, the basis of results is a bit small. Further comparison between geotechnical investigations and geophysical measurements should be completed to get a more comprehensive foundation of data. With more data it is possible to see a clearer trend if the method would work on a large scale or if it seem to be project and soil specific. More in number and frequency of drillings along ERT-profiles will also show not only how the geophysical methods correlate with depth, but also give a better indication on how well the layering provided is homogeneous or not horizontally. In summary the methods used in this project needs to be used more to get a more comprehensive and detailed set of data which will lead to a better founded conclusion.

References

Bazin, S. and A. A. Pfaffhuber (Nov. 1, 2013). "Mapping of quick clay by electrical resistivity tomography under structural constraint". In: *Journal of Applied Geophysics* 98, pp. 280–287. ISSN: 0926-9851. DOI: 10.1016/j.jappgeo.2013.09.002. URL: https://www.sciencedirect.com/science/article/pii/S0926985113001948 (visited on 12/17/2022).

Larsen, Bjørn Eskil (Sept. 12, 2022). *ERT profiles/results*. E-mail.

Long, Michael et al. (Oct. 2012). "Relationship between electrical resistivity and basic geotechnical parameters for marine clays". In: *Canadian Geotechnical Journal* 49.10. Publisher: NRC Research Press, pp. 1158–1168. ISSN: 0008-3674. DOI: 10.1139/t2012-080. URL: https://cdnsciencepub.com/doi/10.1139/t2012-080 (visited on 12/17/2022).

Long, Michael et al. (Feb. 2018). "Glacio-marine clay resistivity as a proxy for remoulded shear strength: correlations and limitations". In: *Quarterly Journal of Engineering Geology and Hydrogeology* 51.1, pp. 63–78. ISSN: 1470-9236, 2041-4803. DOI: 10.1144/qjegh2016-136. URL: https://www.lyellcollection.org/doi/10.1144/qjegh2016-136 (visited on 12/14/2022).

Lundström, K., R. Larsson, and T. Dahlin (Mar. 2009). "Mapping of quick clay formations using geotechnical and geophysical methods". In: *Landslides* 6.1, pp. 1–15. ISSN: 1612-510X, 1612-5118. DOI: 10.1007/s10346-009-0144-9. URL: http://link.springer.com/10.1007/s10346-009-0144-9 (visited on 12/17/2022).

NGF (1982). *VEILEDNING FOR SYMBOLER OG DEFINISJONER I GEOTEKNIKK*.

NGI (Jan. 2023). *NGI - Resistivitetsmålinger - ERT/IP/EM*. NGI. URL: https://www.ngi.no/forskning-og-radgivning/grunnundersokelser-container/geofysiske-grunnundersokelser/resistivitetsmalinger---ertipem/ (visited on 06/18/2023).

Noon, David A., Glen F. Stickley, and Dennis Longstaff (Oct. 1, 1998). "A frequency-independent characterisation of GPR penetration and resolution performance". In: *Journal of Applied Geophysics* 40.1, pp. 127–137. ISSN: 0926-9851. DOI: 10.1016/S0926-9851(98)00008-1. URL: https://www.sciencedirect.com/science/article/pii/S0926985198000081 (visited on 12/05/2022).

NTNU (Oct. 2017). *Geotechnics Field and Laboratory Investigations - course compendium*.

Pfaffhuber, Andreas et al. (Jan. 1, 2016). *In-situ detection of sensitive clays from a geophysical perspective*.

Pfaffhuber, Andreas Aspmo, Sara Bazin, and Tonje E. Helle (2014). "An Integrated Approach to Quick-Clay Mapping Based on Resistivity Measurements and Geotechnical Investigations". In: *Landslides in Sensitive Clays: From Geosciences to Risk Management*. Ed. by Jean-Sébastien L'Heureux et al. Advances in Natural and Technological Hazards Research. Dordrecht: Springer Netherlands, pp. 193–204. ISBN: 978-94-007-7079-9. DOI: 10.1007/978-94-007-7079-9_15. URL: https://doi.org/10.1007/978-94-007-7079-9_15 (visited on 12/17/2022).

Rømoen, M et al. (2010). "Resistivity on marine sediments retrieved from RCPTUsoundings: a Norwegian case study". In.

Solberg, Inger-Lise et al. (Feb. 2008). "Resistivity measurements as a tool for outlining quick-clay extent and valley-fill stratigraphy: a feasibility study from Buvika, central Norway". In: *Canadian Geotechnical Journal* 45.2, pp. 210–225. ISSN: 0008-3674, 1208-6010. DOI: 10.1139/T07-089. URL: http://www.nrcresearchpress.com/doi/10.1139/T07-089 (visited on 12/14/2022).

Solberg, Inger-Lise et al. (Feb. 2012). "Combined geophysical and geotechnical approach to ground investigations and hazard zonation of a quick clay area, mid Norway". In: *Bulletin of Engineering Geology and the Environment* 71.1, pp. 119–133. ISSN: 1435-9529, 1435-9537. DOI: 10.1007/s10064-011-0363-x. URL: http://link.springer.com/10.1007/s10064-011-0363-x (visited on 12/14/2022).

Solberg, Inger-Lise et al. (June 2016). "Geophysical and geotechnical studies of geology and sediment properties at a quick-clay landslide site at Esp, Trondheim, Norway". In: *Engineering Geology* 208, pp. 214–230. ISSN: 00137952. DOI: 10.1016/j.enggeo.2016.04.031. URL: https://linkinghub.elsevier.com/retrieve/pii/S0013795216301247 (visited on 12/14/2022).

Standard Norge (2014). *Geotechnical investigation and testing Laboratory testing of soil Part 1: Determination of water content (ISO 17892-1:2014)*. Standard Norge Report.

— (2017). *Geotechnical investigation and testing Laboratory testing of soil Part 6: Fall cone test (ISO 17892-6:2017)*. Standard Norge Report.

— (2018a). *Geotechnical investigation and testing Laboratory testing of soil Part 12: Determination of liquid and plastic limits (ISO 17892-12:2018)*. Standard Norge Report.

— (2018b). *Geotechnical investigation and testing Laboratory testing of soil Part 7: Unconfined compression test (ISO 17892-7:2017)*. Standard Norge Report.

Statens Vegvesen (July 2022). "V220 Geoteknikk i vegbygging". In: p. 653.

— (Mar. 30, 2023). *CPTu*. Statens vegvesen. URL: https://www.vegvesen.no/fag/teknologi/geofag/geoteknikk/cptu/ (visited on 06/18/2023).

Svoboda, James A. and Richard C. Dorf (2014). *Introduction to electric circuits*. 9th edition. Hoboken, NJ: John Wiley and Sons, Inc. 900 pp. ISBN: 978-1-118-47750-2 978-1-118-52106-9.

With, Christoffer et al. (July 1, 2022). "A methodology for mapping of quick clay in Sweden". In: *Natural Hazards* 112.3, pp. 2549–2576. ISSN: 1573-0840. DOI: 10.1007/s11069-022-05278-y. URL: https://doi.org/10.1007/s11069-022-05278-y (visited on 12/17/2022).

Appendices

A Excel presented results for layering

B ERT-profiles

C Total soundings and CPTUs

D Lab tests location on samples

Appendix A

$$P_1P_2$$

P_5

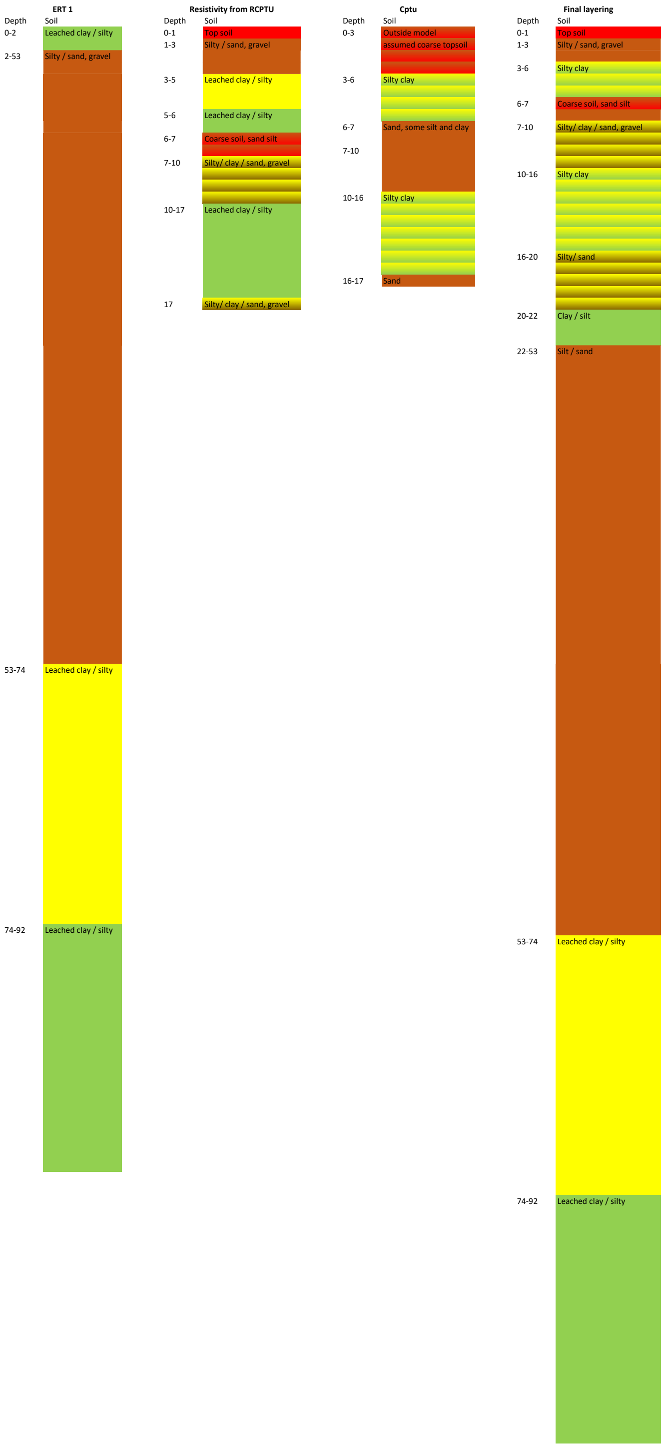

ERT 1
Depth
Soil
0-2
Leached clay / silty
2-53
Silty / sand, gravel
53-74
Leached clay / silty
74-92
Leached clay / silty
Resistivity from RCPTU
Depth
Soil
0-1
Top soil
1-3
Silty / sand, gravel
3-5
Leached clay / silty
5-6
Leached clay / silty
6-7
Coarse soil, sand silt
7-10
Silty/ clay / sand, gravel
10-17
Leached clay / silty
17
Silty/ clay / sand, gravel
Cptu
Depth
Soil
0-3
Outside model
assumed coarse topsoil
3-6
Silty clay
6-7
Sand, some silt and clay
7-10
10-16
Silty clay
16-17
Sand
Final layering
Depth
Soil
0-1
Top soil
1-3
Silty / sand, gravel
3-6
Silty clay
6-7
Coarse soil, sand silt
7-10
Silty/ clay / sand, gravel
10-16
Silty clay
16-20
Silty/ sand
20-22
Clay / silt
22-53
Silt / sand
53-74
Leached clay / silty
74-92
Leached clay / silty

Appendix B

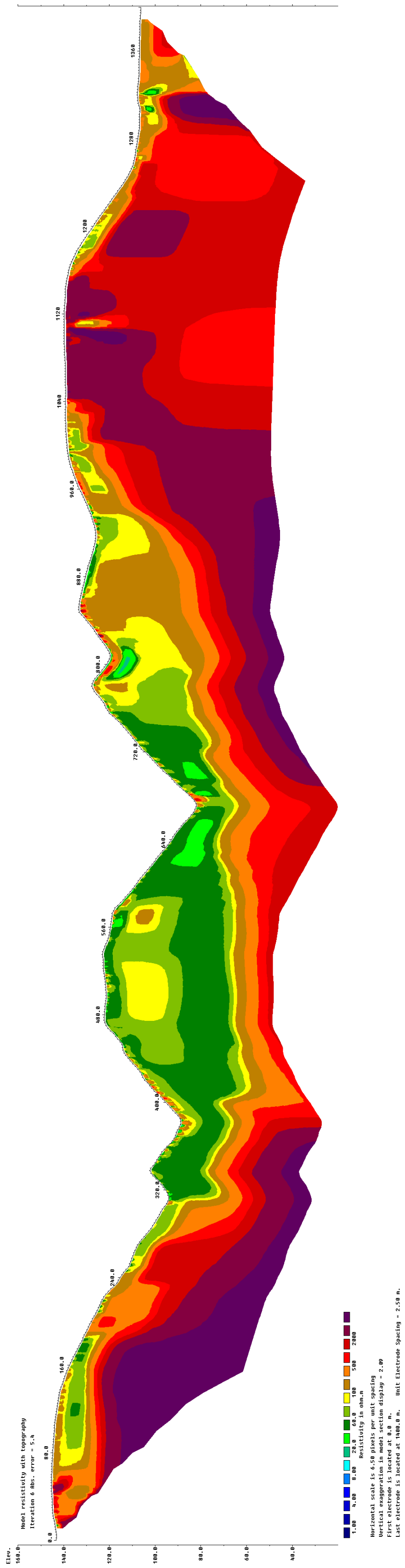

Profile 1

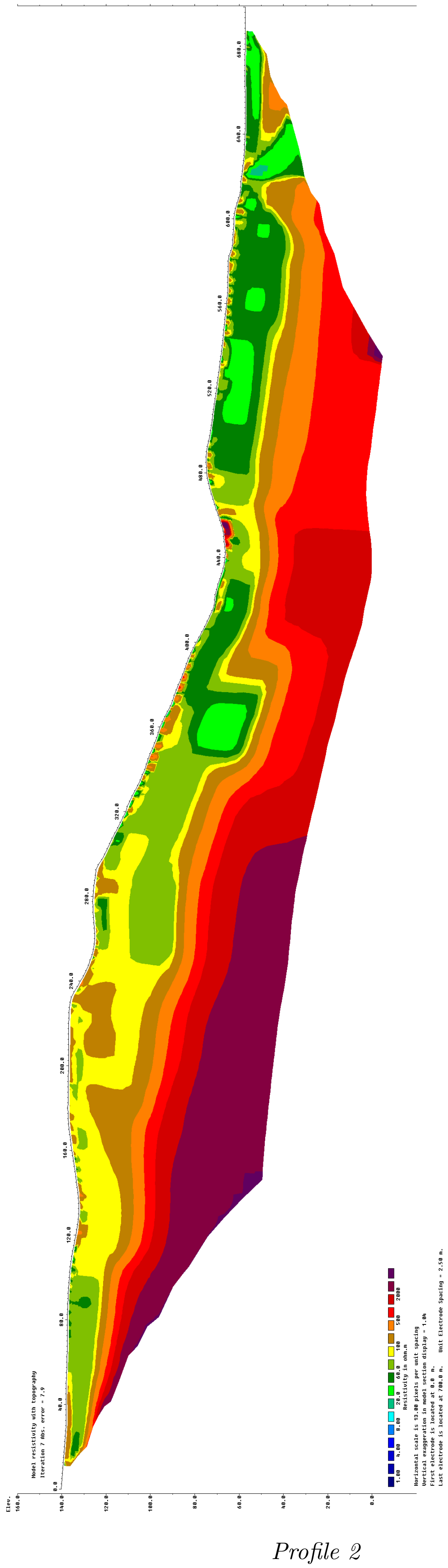

Profile 2

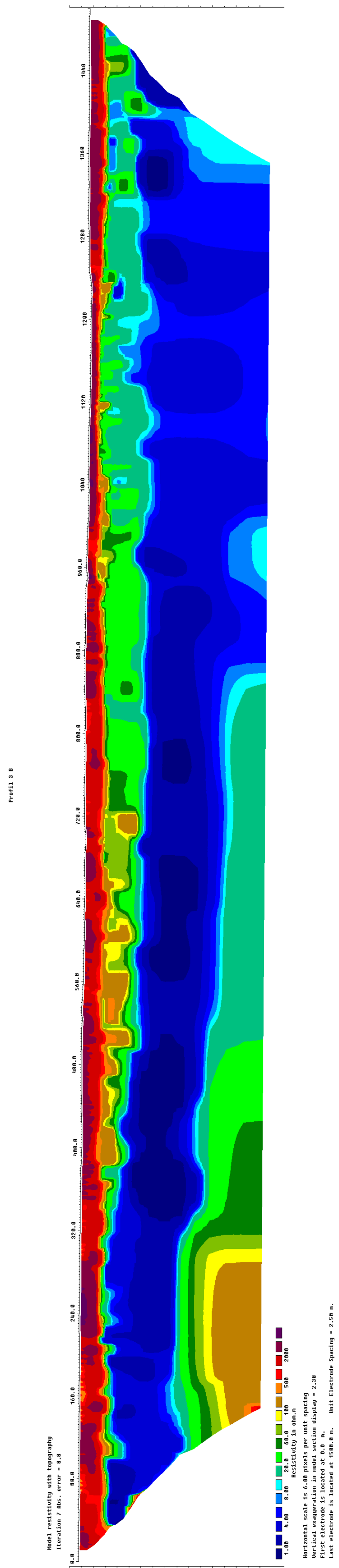

Profile 3

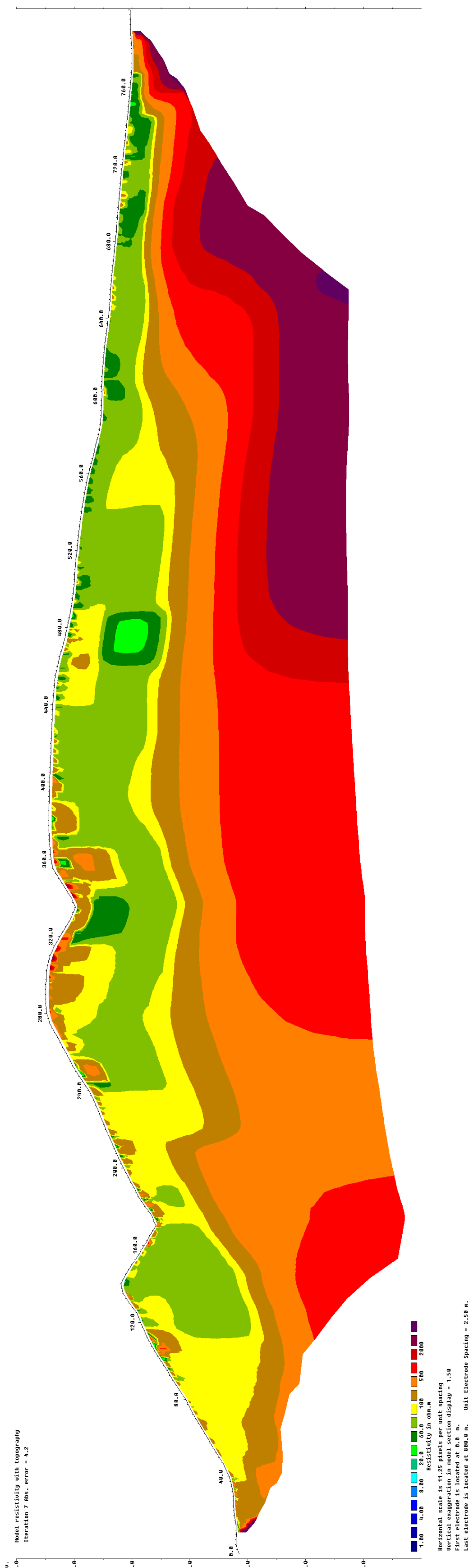

Profile 4

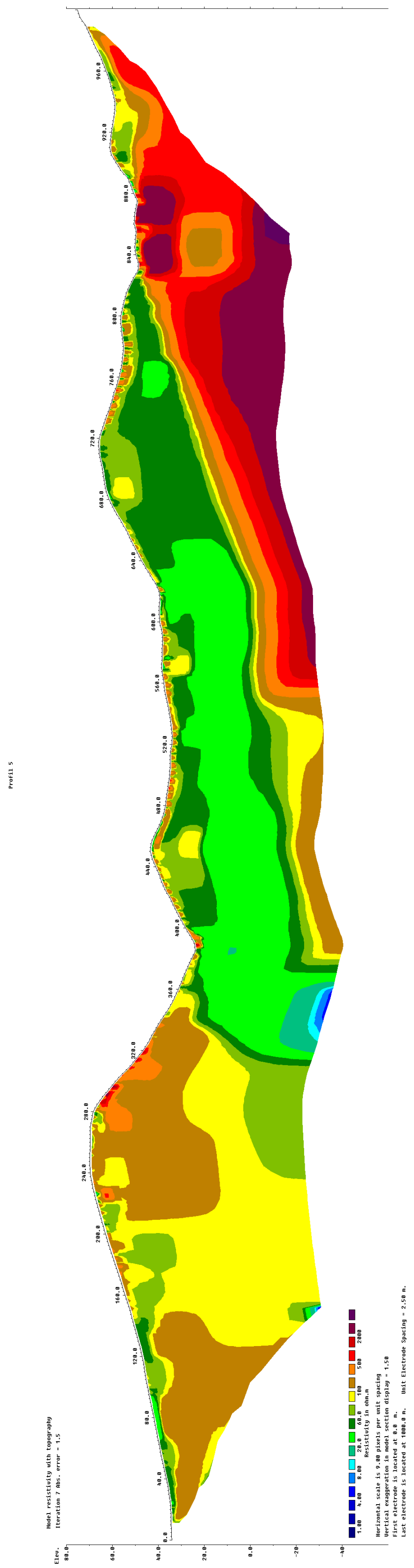

Profile 5

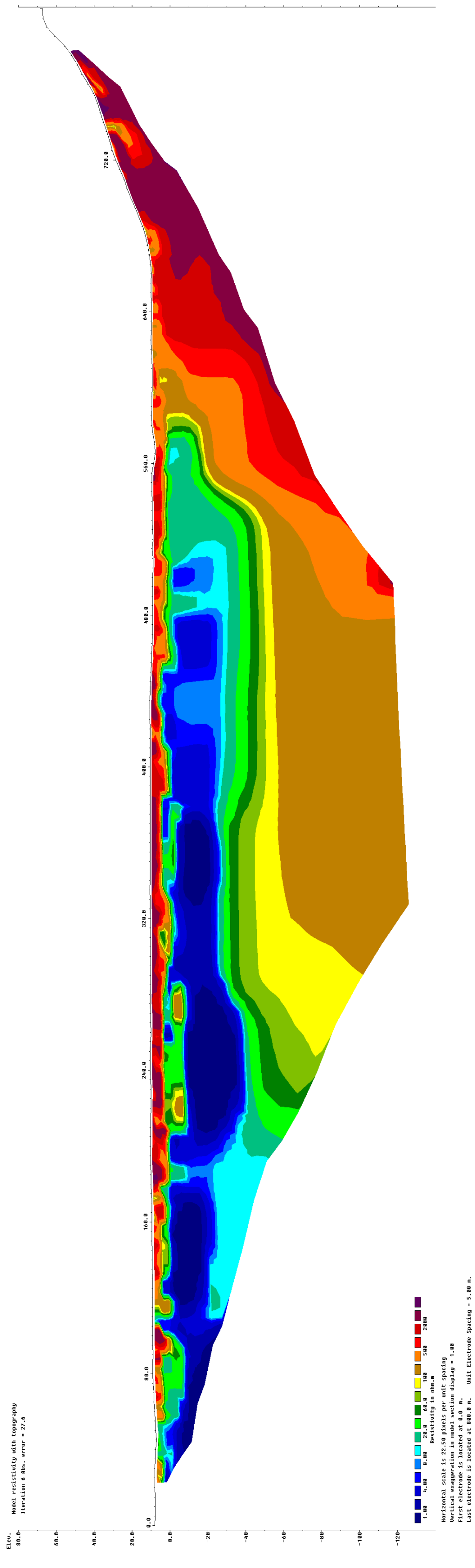

Profile 7

Appendix C

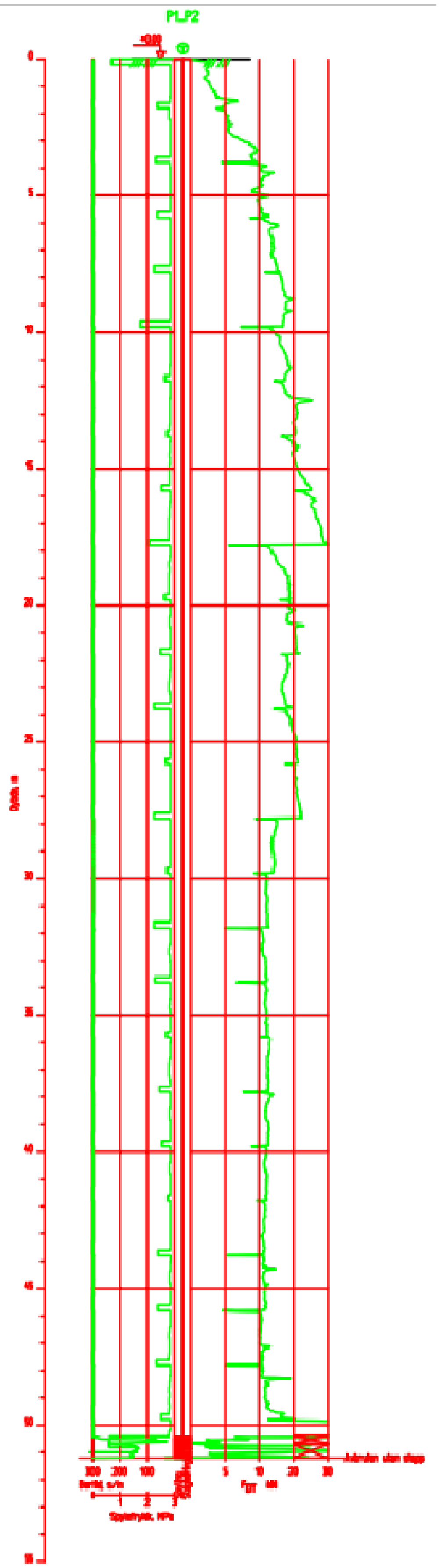

P_1P_2 *total sounding*

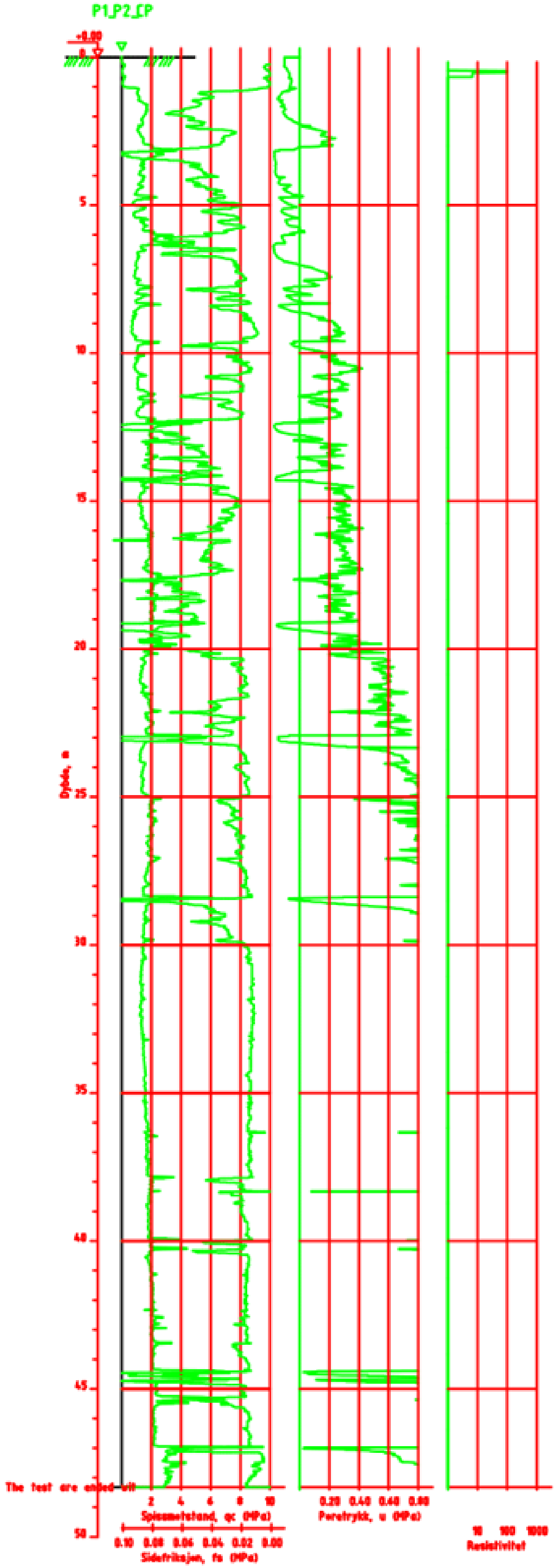

P1_P2_CP
Dybde, m
The test are ended at
Spissmotstand, qc (MPa)
Poretrykk, u (MPa)
Sidefriksjon, fs (MPa)
Resistivitet

P_1P_2 $RCPTU$

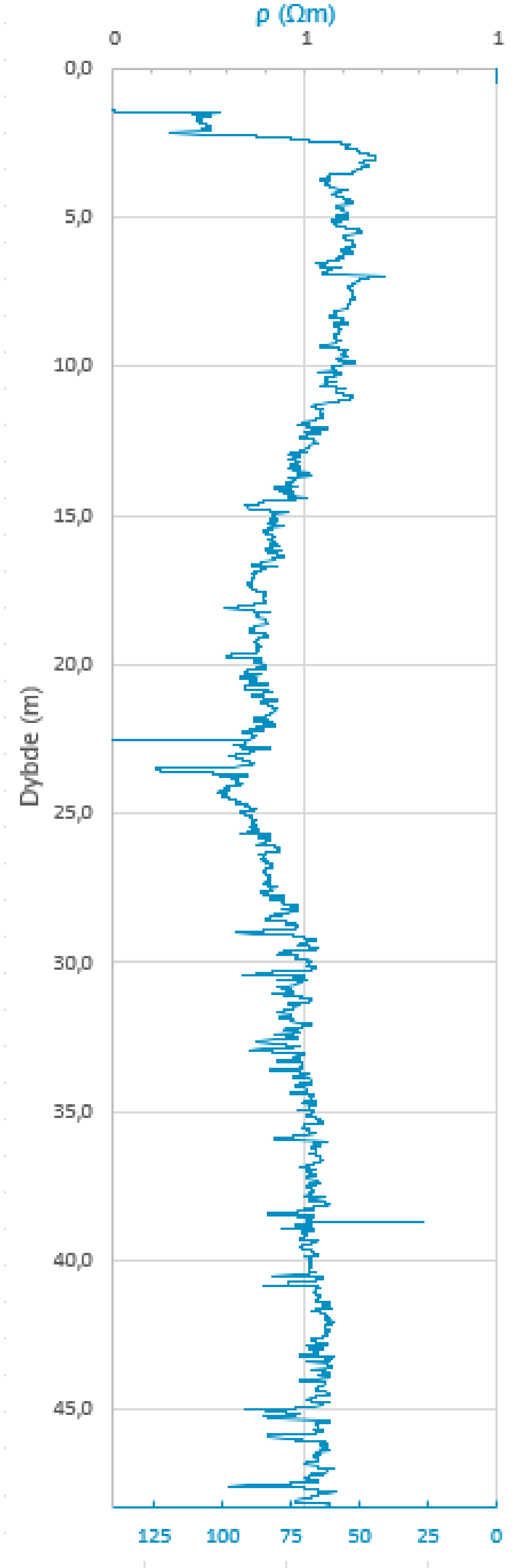

P_1P_2 *resistivity from RCPTU*

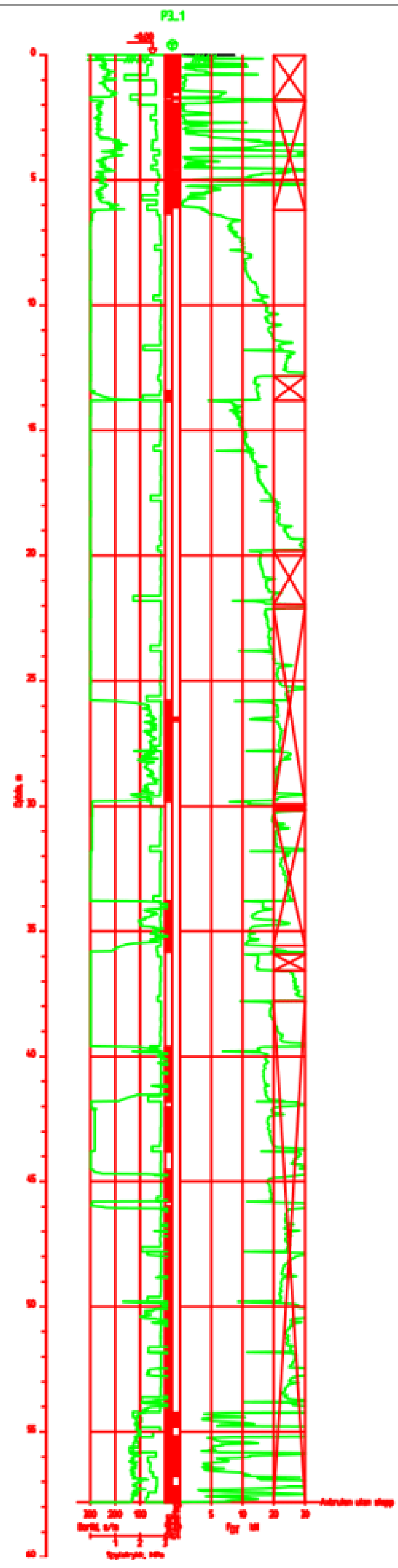

$P3_1$

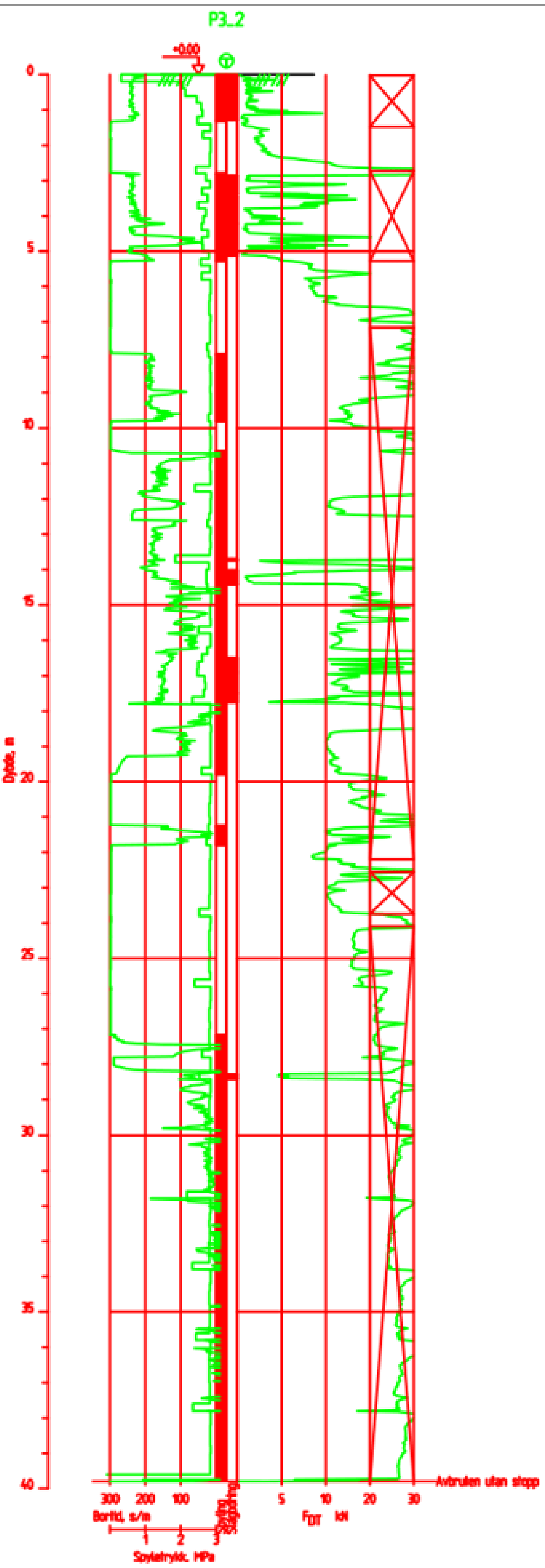
P3_2
+0.00
Dybde, m
0
5
10
15
20
25
30
35
40
Avbrutt uten stopp
300
200
100
Bortid, s/m
1
2
3
Spyletrykk, MPa
5
10
20
30
F_DT kN

$P3_2$

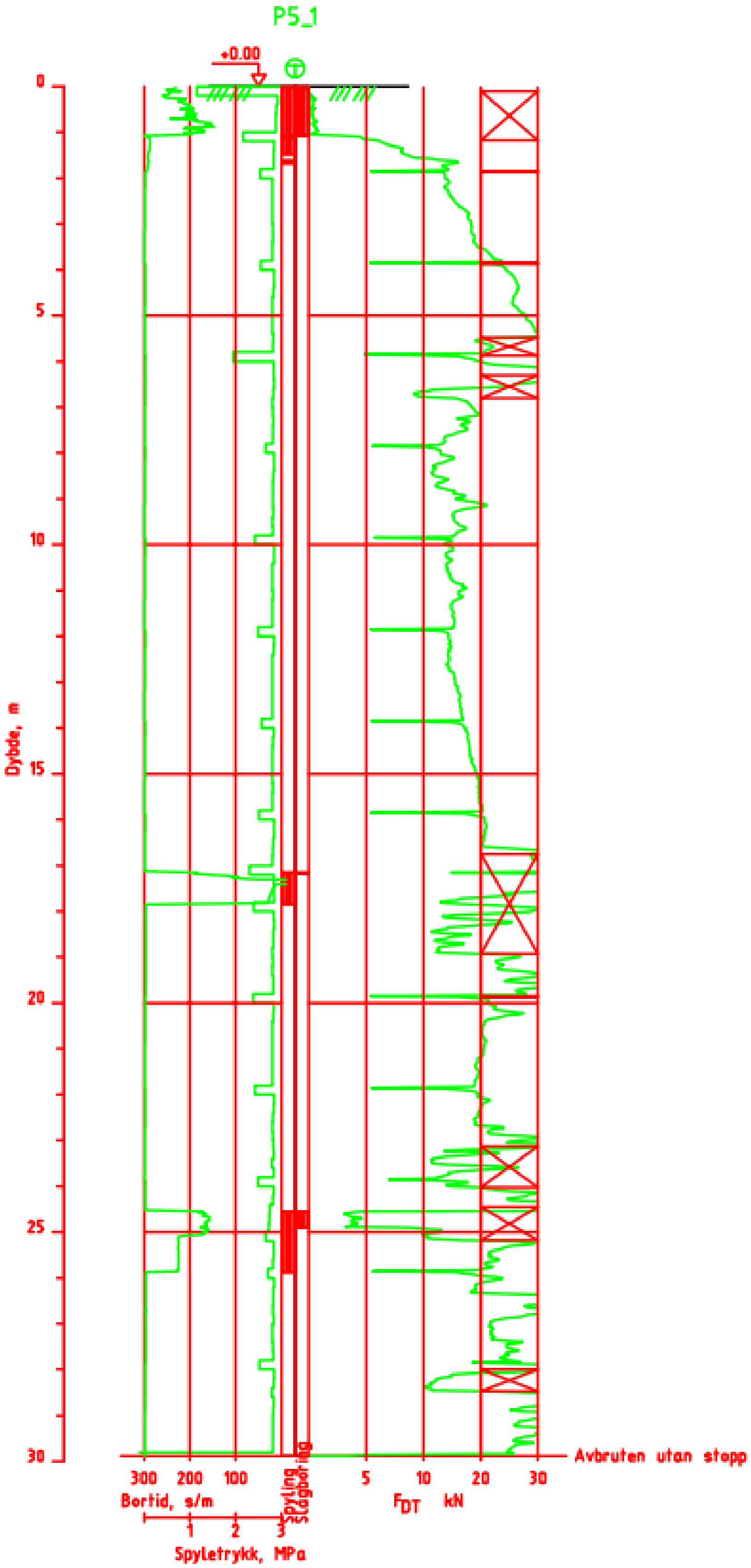

P_5 *total sounding*

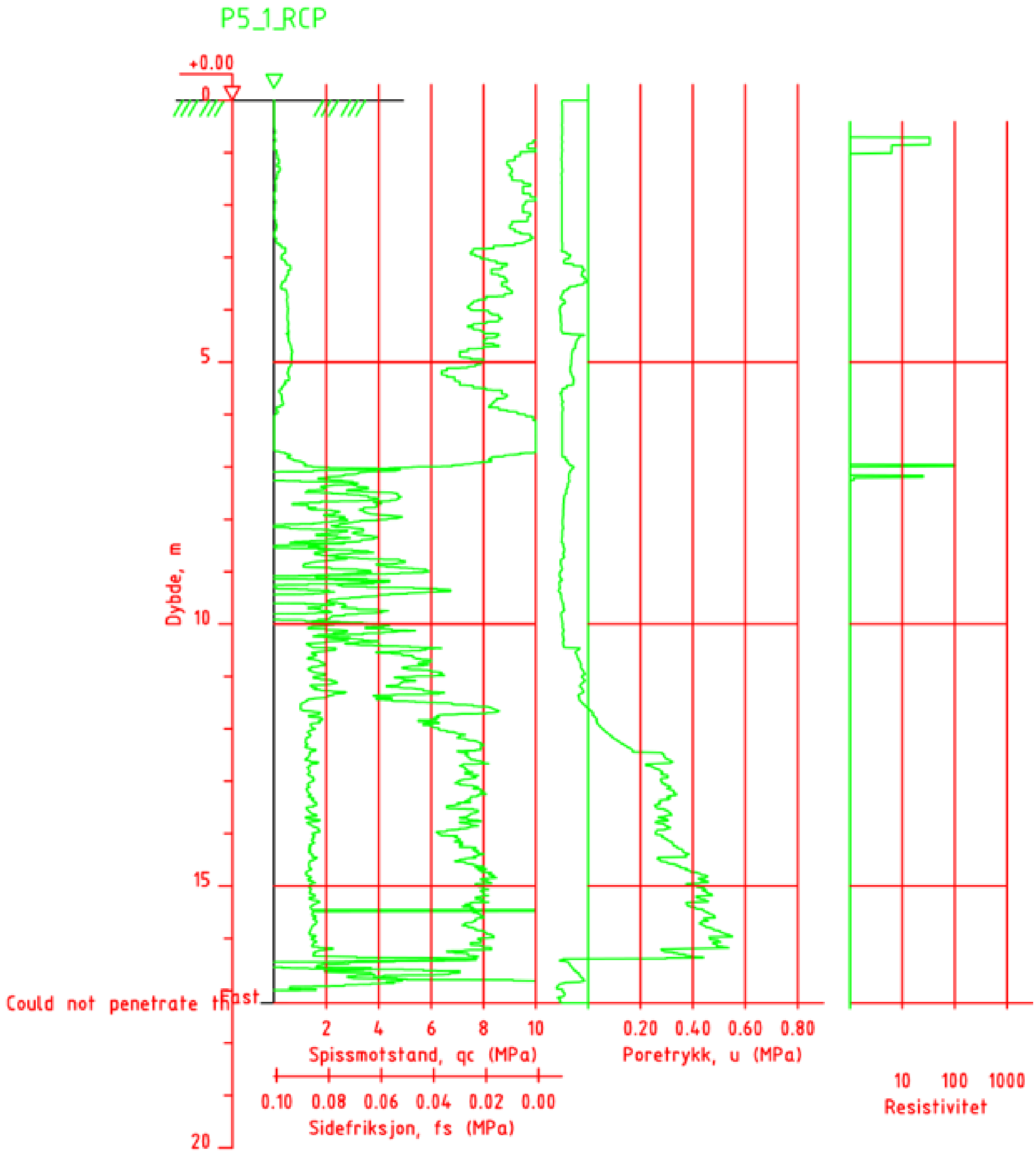
P5_1_RCP
+0.00
0
5
10
15
20
Dybde, m
Could not penetrate th
Fast
2 4 6 8 10
Spissmotstand, qc (MPa)
0.10 0.08 0.06 0.04 0.02 0.00
Sidefriksjon, fs (MPa)
0.20 0.40 0.60 0.80
Poretrykk, u (MPa)
10 100 1000
Resistivitet

P_5 *RCPTU*

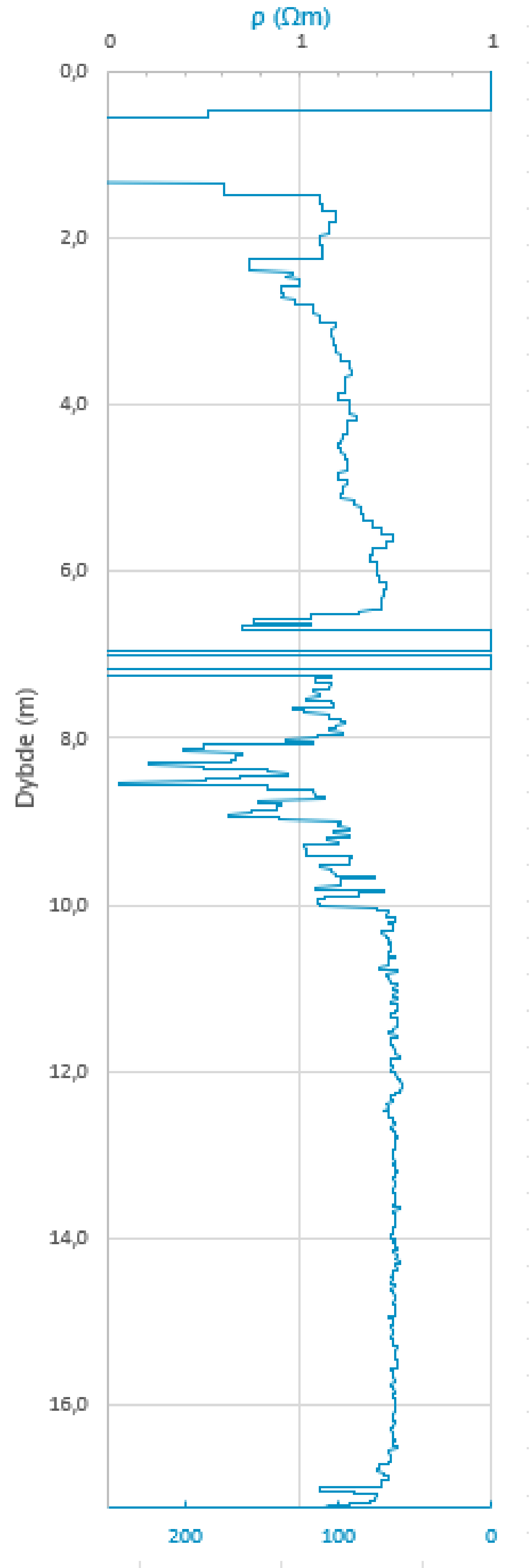

P_5 resistivity from RCPTU

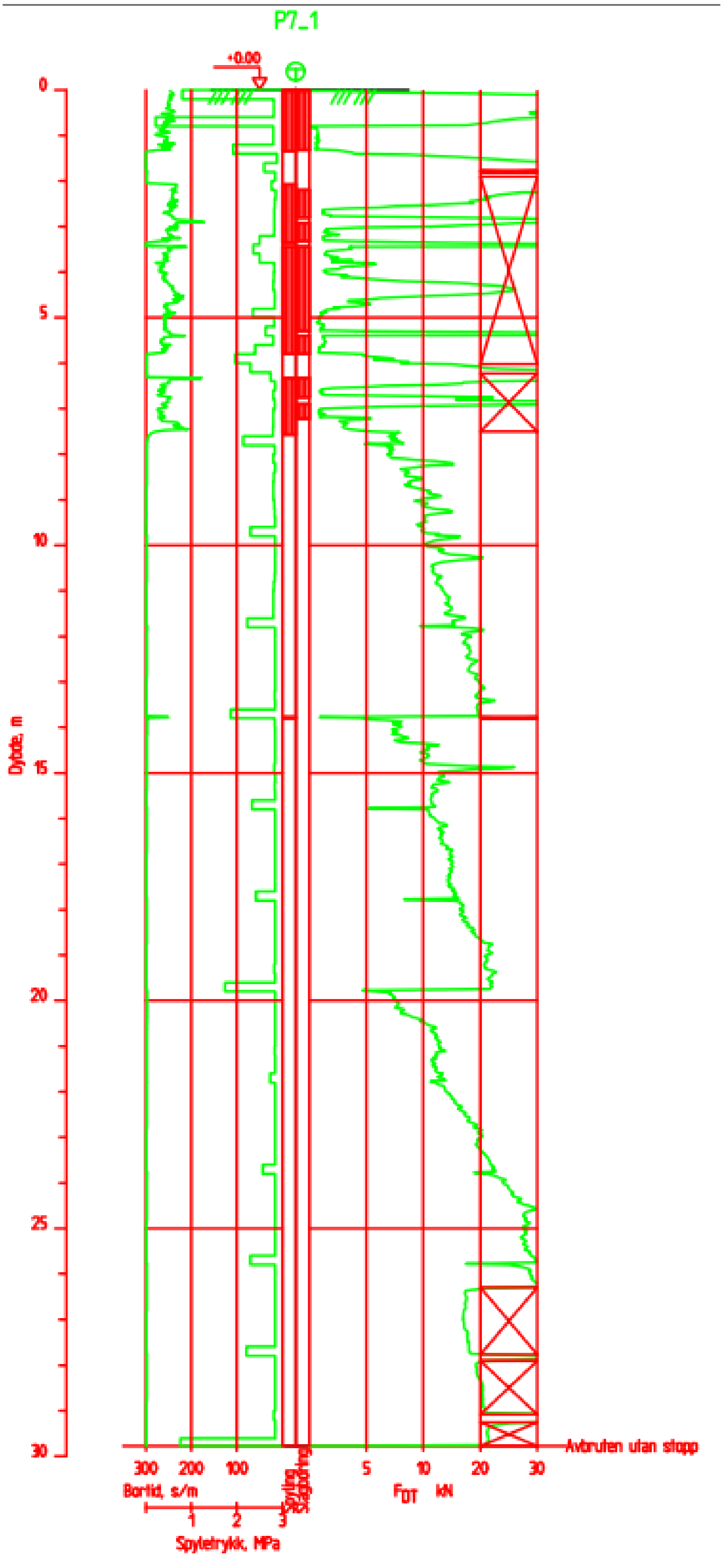
P7_1
+0.00
Dybde, m
0
5
10
15
20
25
30
Avbruten utan stopp
300
200
100
Bortid, s/m
1
2
3
Spyletrykk, MPa
Spyling
Slagboring
5
10
20
30
F_{DT} kN

$P7_1$

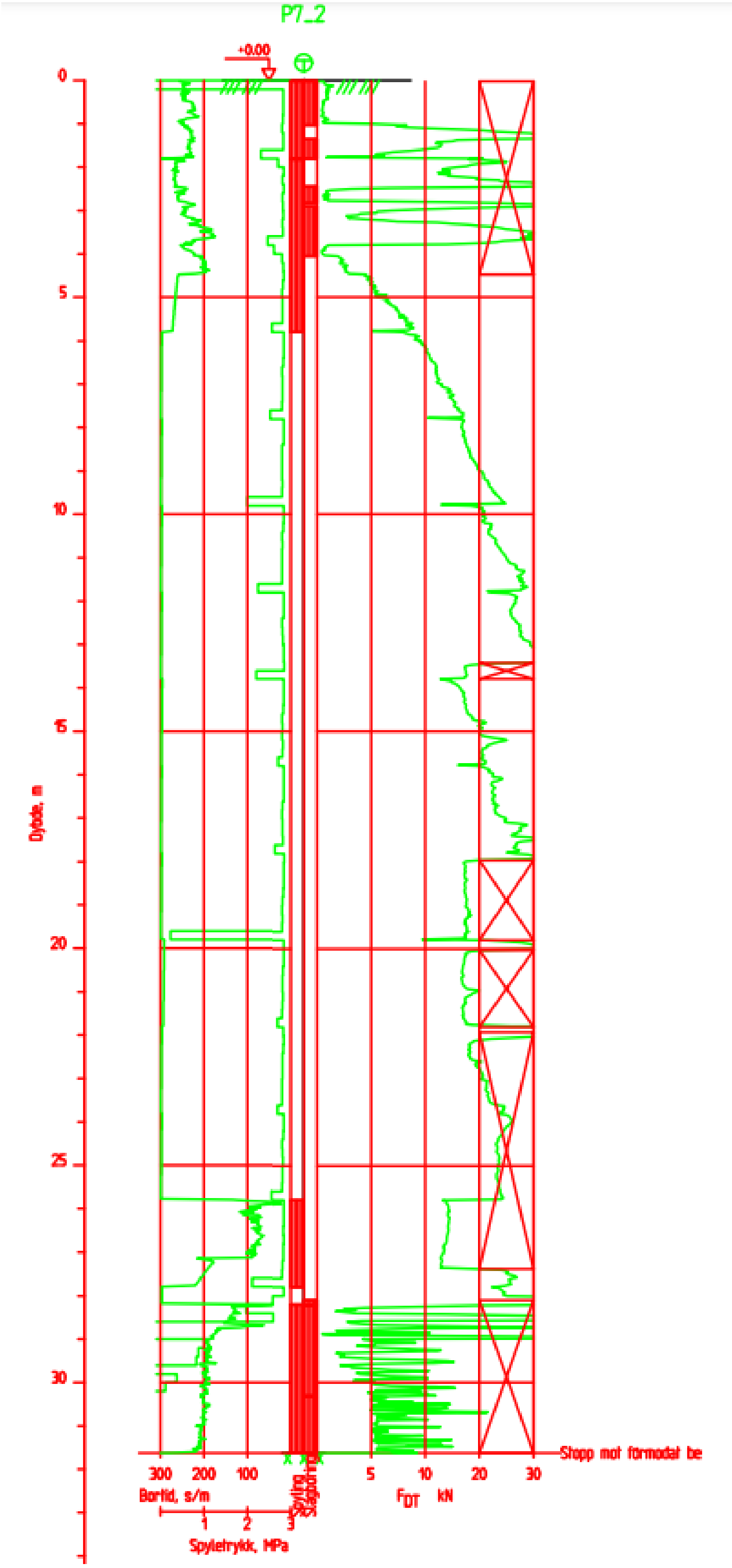
P7_2
+0.00
0
5
10
15
20
25
30
Dybde, m
300
200
100
Borlid, s/m
1
2
3
Spyletrykk, MPa
Spyling
Slagboring
5
10
20
30
F_DT kN
Stopp mot formodat be

$P7_2$

Appendix D

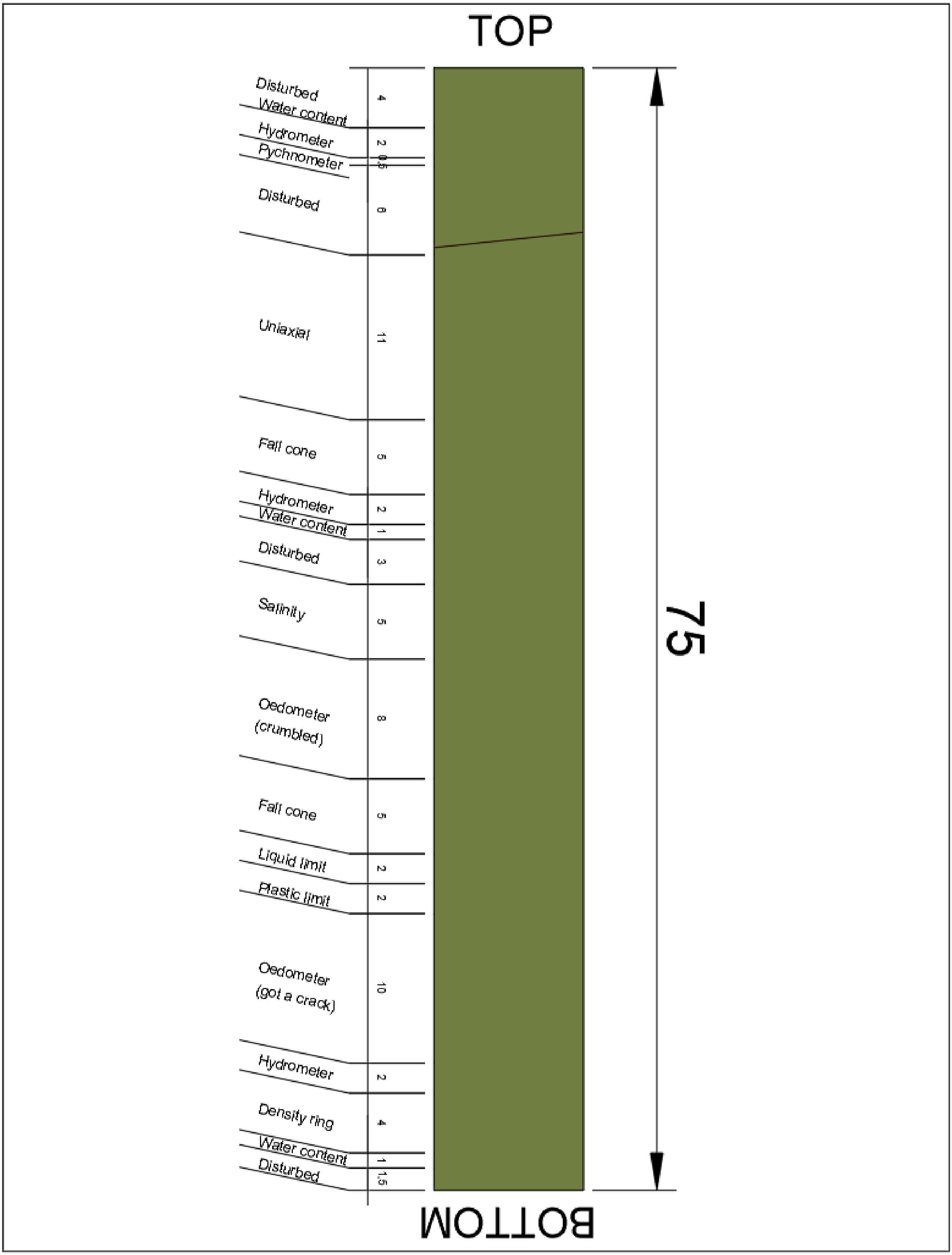

Sample 1

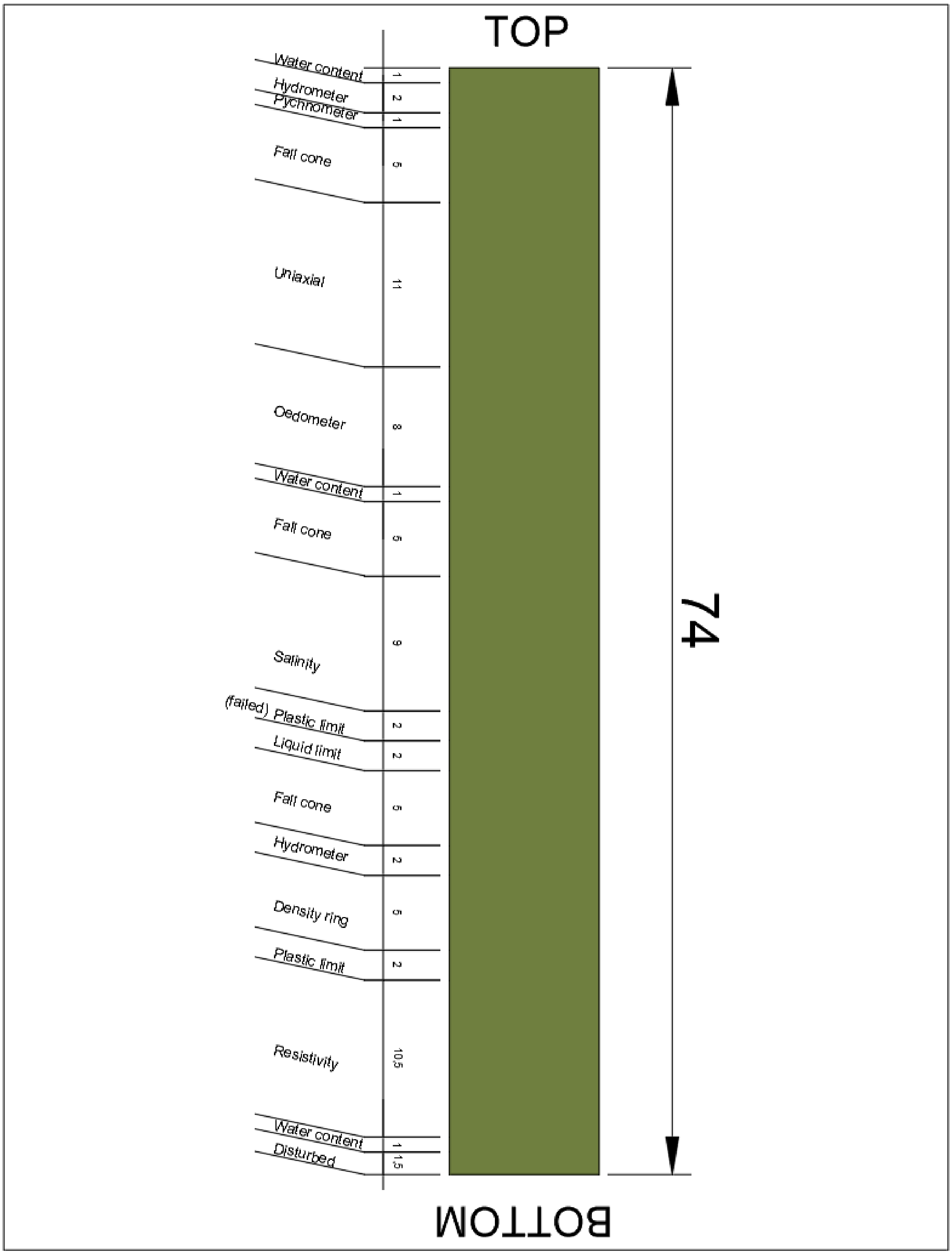
TOP
Water content
Hydrometer
Pychnometer
Fall cone
Uniaxial
Oedometer
Water content
Fall cone
Salinity
(failed) Plastic limit
Liquid limit
Fall cone
Hydrometer
Density ring
Plastic limit
Resistivity
Water content
Disturbed
74

Sample 2

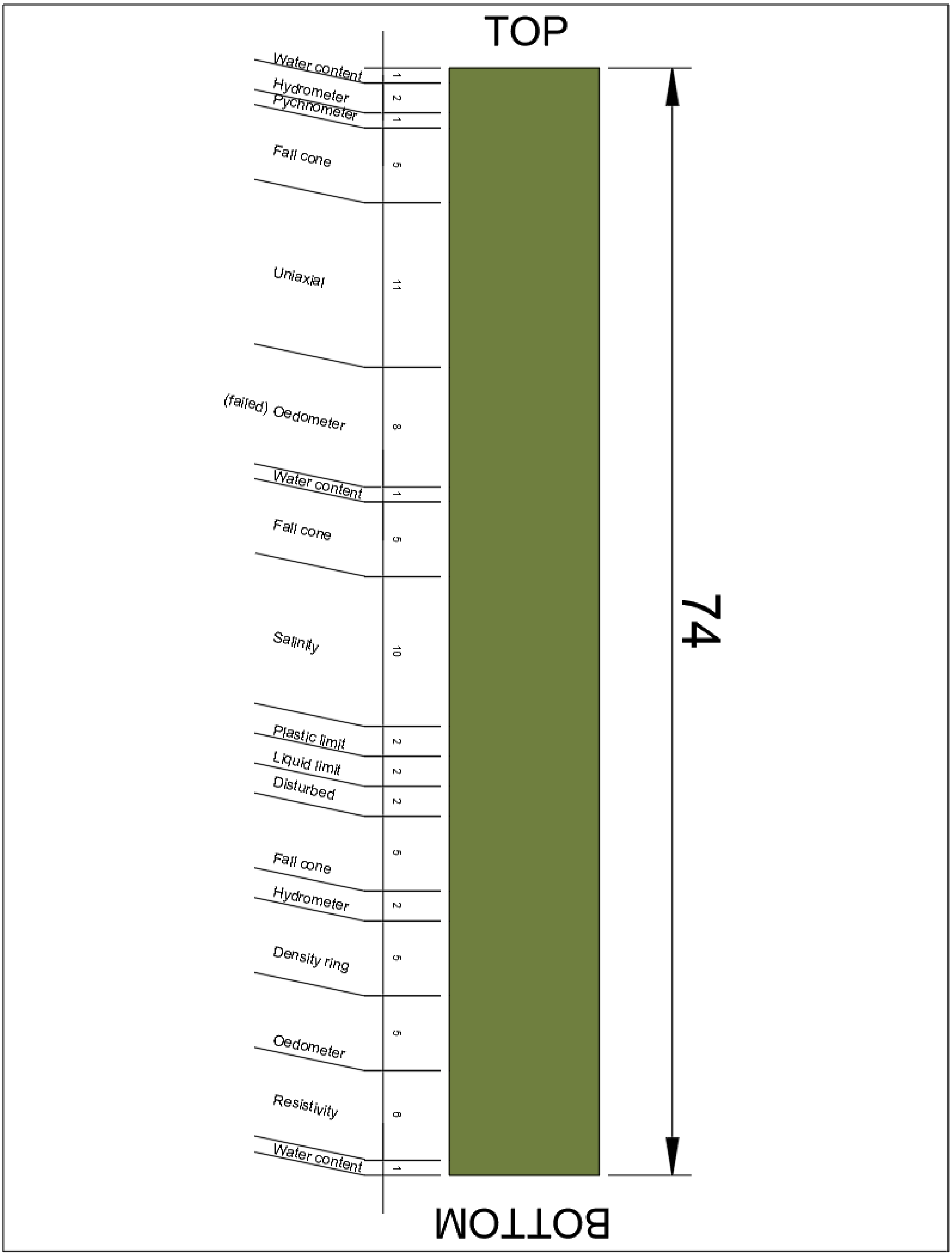
TOP
Water content
1
Hydrometer
2
Pychnometer
1
Fall cone
5
Uniaxial
11
(failed) Oedometer
8
Water content
1
Fall cone
5
Salinity
10
Plastic limit
2
Liquid limit
2
Disturbed
2
5
Fall cone
2
Hydrometer
2
Density ring
5
5
Oedometer
Resistivity
8
Water content
1
74
BOTTOM

Sample 3

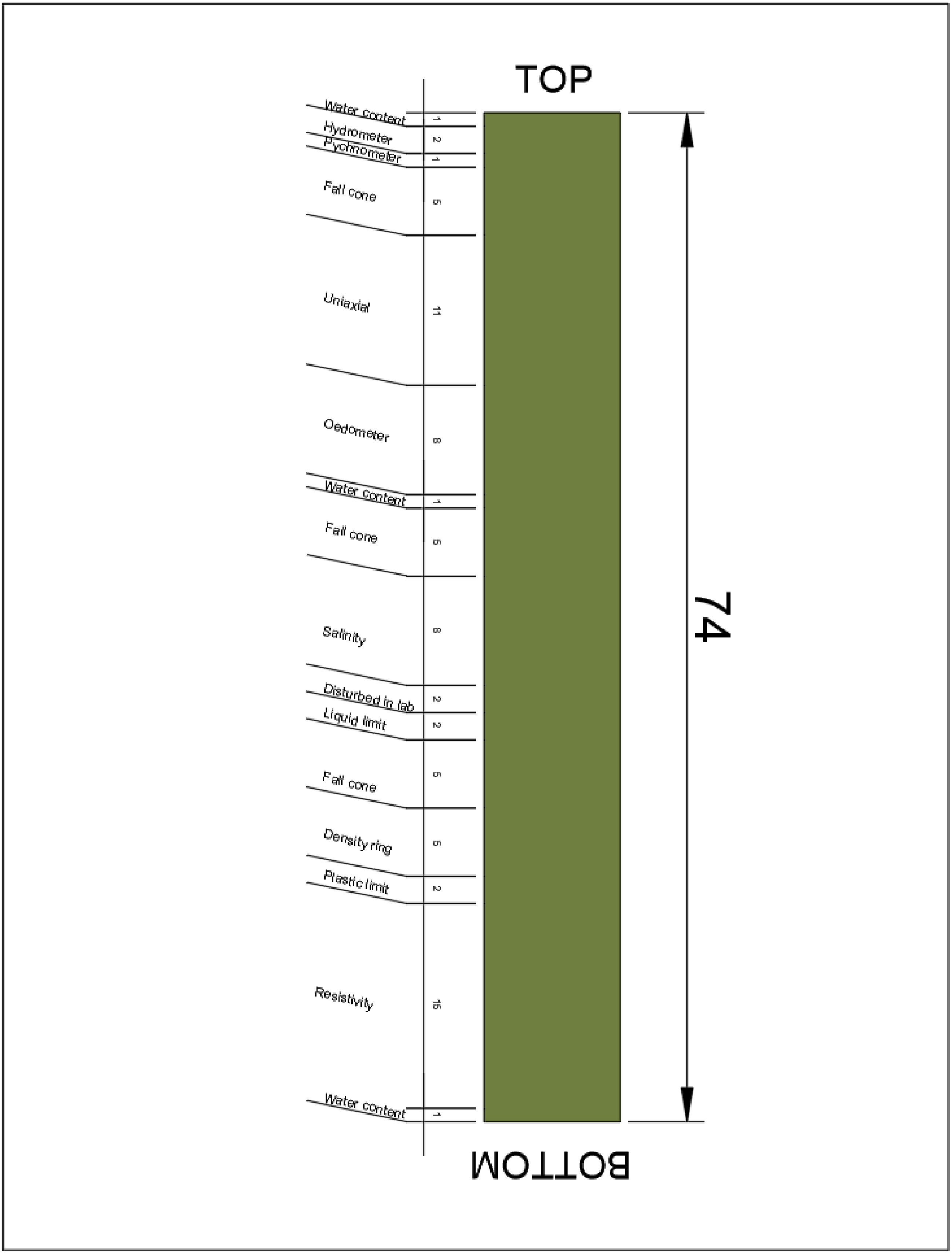
TOP
Water content 1
Hydrometer 2
Pycnometer 1
Fall cone 5
Uniaxial 11
Oedometer 8
Water content 1
Fall cone 5
Salinity 8
Disturbed in lab 2
Liquid limit 2
Fall cone 5
Density ring 5
Plastic limit 2
Resistivity 15
Water content 1
74
BOTTOM

Sample 4

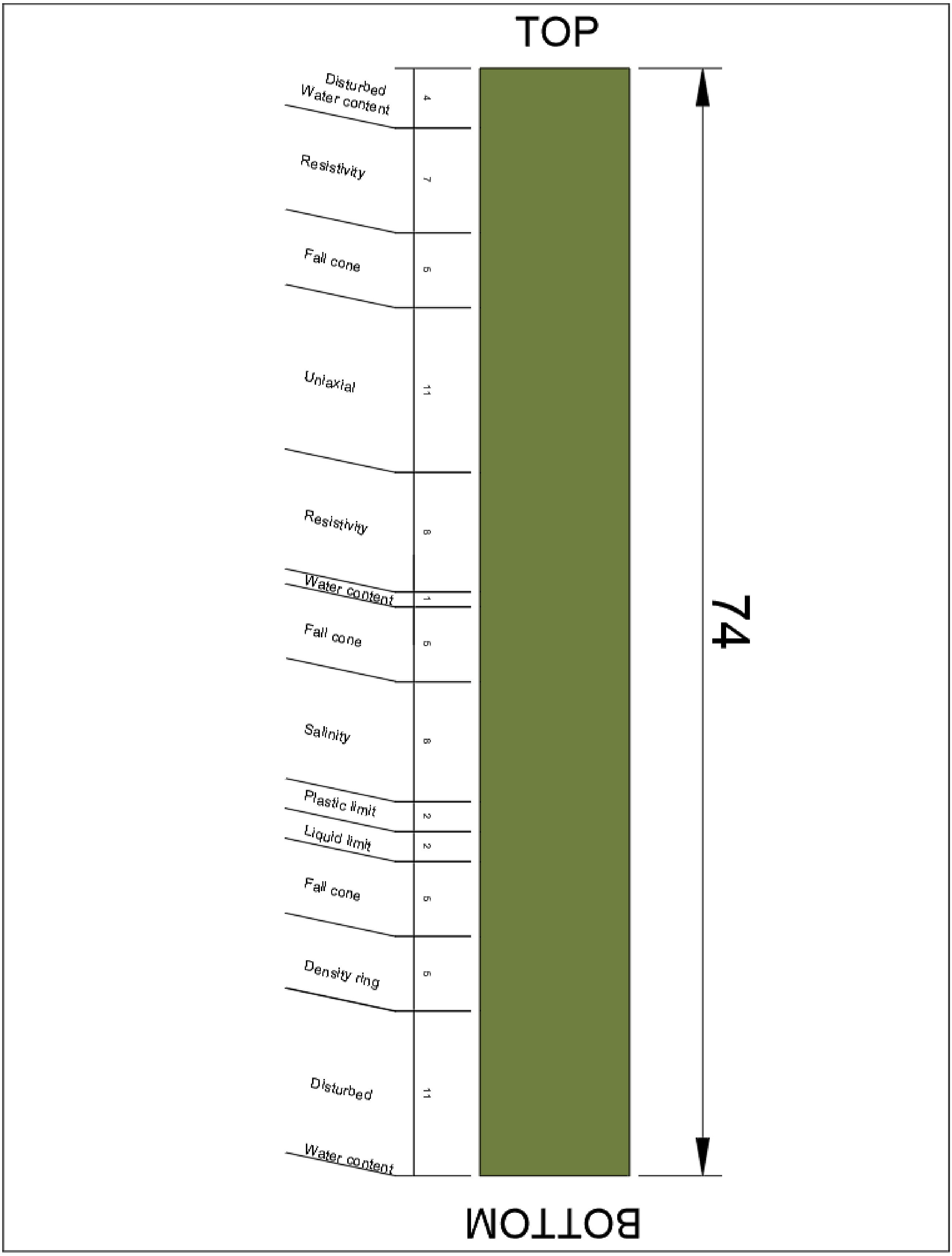
TOP
Disturbed
Water content
4
Resistivity
7
Fall cone
5
Uniaxial
11
Resistivity
8
Water content
1
Fall cone
5
Salinity
8
Plastic limit
2
Liquid limit
2
Fall cone
5
Density ring
5
Disturbed
Water content
11
74
BOTTOM

Sample 5

NTNU

Norwegian University of
Science and Technology